NASA
Technical
Paper
2215

January 1984

Buckling Loads of Stiffened Panels Subjected to Combined Longitudinal Compression and Shear: Results Obtained With PASCO, EAL, and STAGS Computer Programs

W. Jefferson Stroud,
William H. Greene,
and Melvin S. Anderson

NASA

NASA
Technical
Paper
2215

1984

Buckling Loads of Stiffened Panels Subjected to Combined Longitudinal Compression and Shear: Results Obtained With PASCO, EAL, and STAGS Computer Programs

W. Jefferson Stroud,
William H. Greene,
and Melvin S. Anderson

Langley Research Center
Hampton, Virginia

National Aeronautics
and Space Administration

**Scientific and Technical
Information Office**

1984

CONTENTS

SUMMARY

The report examines several buckling analysis procedures for stiffened panels, presents accurate results for seven stiffened panels, and illustrates buckling modes with plots of buckling mode shapes. All panels are rectangular and have stiffeners in one direction - down the length of the panel.

The buckling analyses used in PASCO are summarized with emphasis placed on the shear buckling analyses. PASCO buckling analyses include the basic VIPASA analysis, which is essentially exact for longitudinal and transverse loads, and a smeared stiffener solution (equivalent orthotropic plate solution) that was added in an attempt to alleviate a shortcoming in the VIPASA analysis - underestimation of the shear buckling load for modes having a buckling half-wavelength equal to the panel length. Such buckling modes are sometimes referred to as overall modes or general instability modes. Buckling results are then presented for seven stiffened panels loaded by combinations of longitudinal compression and shear. The buckling results were obtained with the PASCO, EAL, and STAGS computer programs. The EAL and STAGS solutions were obtained with a fine finite element mesh and are very accurate. These finite element solutions together with the PASCO results for pure longitudinal compression provide benchmark calculations to evaluate other analysis procedures. For each example, several figures illustrate buckling mode shapes for pure compression and pure shear loadings. It was concluded that the smeared stiffener solution should be used only with caution.

INTRODUCTION

Although buckling analysis procedures that are both fast and accurate have been developed for stiffened panels subjected to longitudinal (N_x) and transverse (N_y) loadings (for example, VIPASA, refs. 1 to 3, and BUCLASP2, ref. 4), no such procedure has been developed for analyzing stiffened panels subjected to loadings involving shear (N_{xy}). (See fig. 1.) VIPASA nearly meets the dual objectives of speed and accuracy; however, when the loading involves shear, VIPASA underestimates the buckling load for the overall mode - that is, the mode for which the buckling half-wavelength in the direction of the stiffeners is equal to the panel length. VIPASA is generally accurate for loadings involving shear when the buckling half-wavelength in the direction of the stiffeners is less than one-third the panel length.

Shear buckling analysis procedures in current use include the following modeling approaches: stiffeners modeled as linked plates with infinite panel length (VIPASA, ref. 1); hinges along plate element connections for local buckling and smeared stiffnesses for overall buckling (for example, ref. 5); approximations in which stiffeners are modeled as discrete lines of bending (EI) and twisting (GJ) stiffnesses on the panel skin; and general purpose finite element approaches (for example, EAL, refs. 6 and 7, and STAGS, refs. 8 and 9). All these

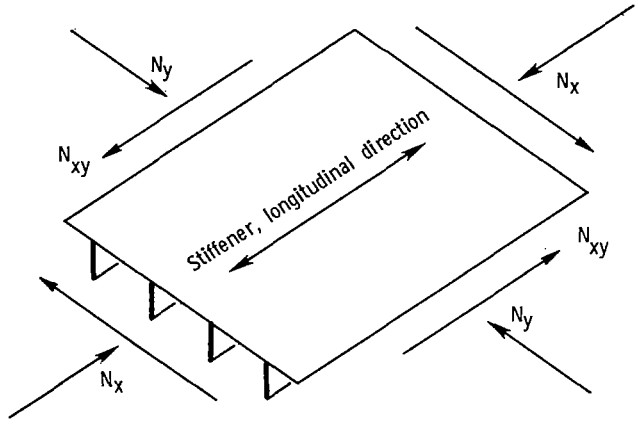

Figure 1.- Loadings and orientations.

approaches have shortcomings. The shortcoming of the approach used in VIPASA is mentioned in the previous paragraph and is discussed in this report. When stiffnesses are smeared, local deformations that contribute to the overall buckling mode are lost. Some local deformations are also lost when the stiffeners are modeled as EI and GJ stiffeners. Finite element approaches can provide high accuracy by using detailed modeling and fine meshes; however, to obtain accurate results, the computation costs may be high.

Because of the shortcomings in VIPASA, the buckling analysis in PASCO (refs. 10 to 13), an alternate solution approach for predicting overall shear buckling was explored and incorporated in PASCO. That approach is based on smeared orthotropic stiffnesses.

This report presents buckling results obtained with the computer programs PASCO (which includes both VIPASA and a smeared orthotropic solution), EAL, and STAGS for seven stiffened panels. For each panel, results are presented for several combinations of inplane shear and longitudinal (stiffener direction) compression ranging from pure shear to pure longitudinal compression. The results serve three purposes. They help evaluate the shear buckling analyses in PASCO, they provide accurate benchmark calculations to evaluate other analysis procedures, and they help provide a better understanding of the buckling mechanism for stiffened panels through the numerous detailed plots of buckling mode shapes.

SYMBOLS

Values are given in both SI and U.S. Customary Units. The calculations were made in U.S. Customary Units.

b plate width

D plate bending stiffness

D_{11}, D_{22}, D_{33} orthotropic stiffnesses defined in equation (2)

E Young's modulus

E_1, E_2 Young's modulus of composite material in fiber direction and transverse to fiber direction, respectively

E_{12} shear modulus of composite material in coordinate system defined by fiber direction

EI bending stiffness of beam

e amplitude of bow-type imperfection at panel midlength

GJ twisting stiffness of beam

L panel length

M_x bending moment about line parallel to Y-axis (see fig. 2)

M_y bending moment about line parallel to X-axis

N_x applied longitudinal compressive loading per unit length (see fig. 2)

$N_{x_{cr}}$ value of N_x that causes buckling

N_{xy} applied shear loading per unit length (see fig. 2)

$N_{xy_{cr}}$ value of N_{xy} that causes buckling

N_y applied transverse loading per unit length (see fig. 2)

P lateral pressure

u,v,w buckling displacements

W panel width

X,Y,Z coordinate axes in longitudinal, transverse, and lateral directions, respectively

x,y,z coordinates

ϵ_x strain in x-direction

θ fiber orientation angle (see fig. 9)

λ buckling half-wavelength

μ Poisson's ratio

μ_1, μ_2 Poisson's ratios of composite material in coordinate system defined by fiber direction, $\mu_1 = \mu_2 \frac{E_1}{E_2}$

Abbreviations:

Anti indicates that buckling displacement w is antisymmetric with respect to a point at the center of the panel

FACTOR eigenvalue, the product of FACTOR and applied load is buckling load

S.S. simple support boundary conditions

Sym indicates that buckling displacement w is symmetric with respect to a point at the center of the panel

Computer programs:

BUCLASP2 BUCkling of LAminated Stiffened Panels

EAL Engineering Analysis Language

PASCO Panel Analysis and Sizing COde

STAGS STructural Analysis of General Shells

VIPASA Vibration and Instability of Plate Assemblies including Shear and Anisotropy

BUCKLING ANALYSIS IN PASCO FOR LOADINGS INVOLVING SHEAR

PASCO is a computer program for analyzing and sizing uniaxially stiffened composite panels subject to the loadings shown in figure 2. PASCO is described in references 10 to 13.

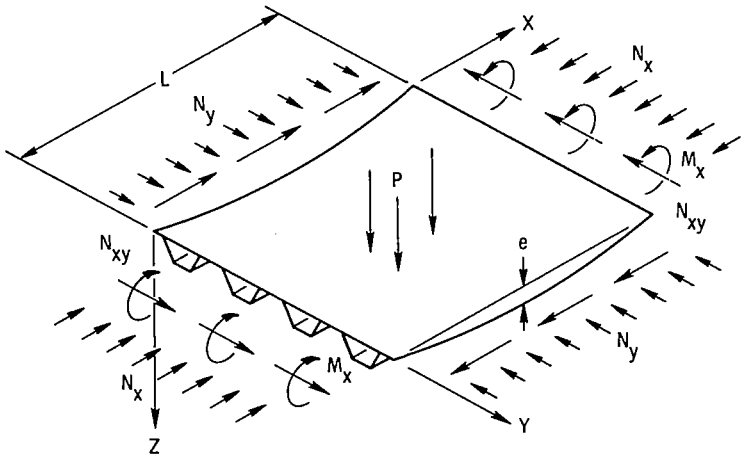

Figure 2.- Stiffened panel with initial bow, applied loading, and coordinate system.

As pointed out in the introduction, an important limitation of PASCO is that VIPASA (the buckling analysis in PASCO) underestimates the buckling load when the loading involves shear and the buckle mode is a general or overall skewed mode having a longitudinal buckle length equal to the length of the panel. That limitation and an approximate analysis technique intended to overcome it are discussed in this section.

VIPASA Buckling Analysis

VIPASA, the buckling analysis program incorporated in PASCO, treats an arbitrary assemblage of plate elements with each plate element i loaded by $(N_x)_i$, $(N_y)_i$, and $(N_{xy})_i$. The buckling analysis connects the individual plate elements and maintains continuity of the buckle pattern across the intersection of neighboring plate elements. The buckling displacement w assumed in VIPASA for each plate element is of the form

$$w = f_1(y) \cos \frac{\pi x}{\lambda} - f_2(y) \sin \frac{\pi x}{\lambda} \tag{1}$$

where λ is the buckling half-wavelength. Similar expressions are assumed for the inplane displacements u and v. Because the buckling displacements are assumed to have a specified form in the x-direction, the VIPASA solution is essentially a one-dimensional solution. (The finite element solutions discussed subsequently are two-dimensional.) The functions $f_1(y)$ and $f_2(y)$ satisfy the differential equation of equilibrium and allow various boundary conditions to be prescribed on the lateral edges of the panel. Boundary conditions cannot be prescribed on the ends of the panel. However, certain useful boundary conditions are implicitly satisfied at the ends of the panel. VIPASA is, therefore, still effective for analyzing a broad spectrum of structural analysis problems. Boundary conditions at the ends of the panel

and the effect of these boundary conditions on the predicted buckling load are discussed in the following paragraphs.

For orthotropic plate elements with no shear loading, the solution given by equation (1) involves a series of node lines that are straight, perpendicular to the longitudinal panel axis, and spaced λ apart, as shown in figure 3. Along each of these node lines, the buckling displacements satisfy simple support conditions. Therefore, for values of λ given by $\lambda = L, L/2, L/3, \ldots, L/m$, where m is an integer and L is the panel length, the nodal pattern shown in figure 3 satisfies simple support boundary conditions at the ends of a finite, rectangular, stiffened panel. For this case, the VIPASA solution is exact.

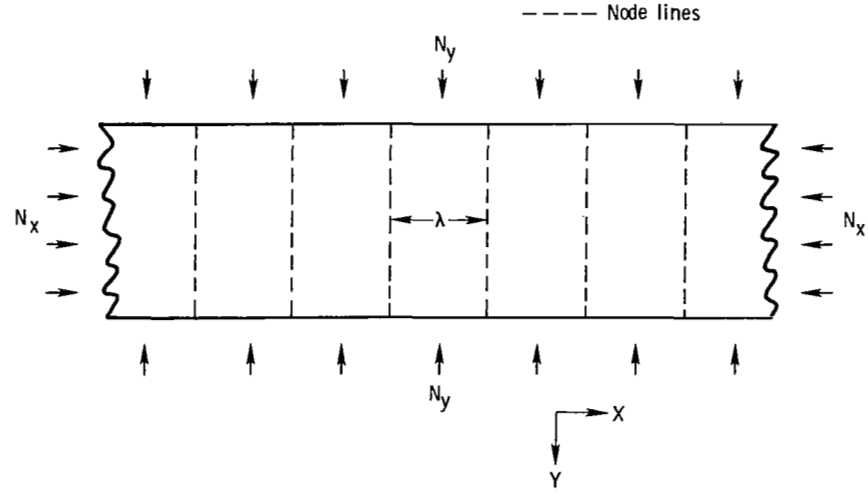

Figure 3.- Node lines for orthotropic plate elements with no shear loading.

For anisotropic plate elements and/or plate elements with a shear loading, the solution given by equation (1) involves node lines that are skewed and not straight, but the node lines are still spaced λ apart, as shown in figure 4. (Because anisotropy generally has negligible effect on buckling loads for long-wavelength buckling modes and because it is these long-wavelength modes that are troublesome, reference to anisotropy is dropped in the following discussion.) Since node lines cannot coincide with the ends of the rectangular panel, the VIPASA solution for loadings involving shear is accurate only when many buckles form along the panel length, in which case boundary conditions at the ends are not important. An example in which $\lambda = L/4$ is shown in figure 5.

As λ approaches L, the VIPASA buckling analysis for a panel loaded by N_{xy} may underestimate the buckling load substantially. One explanation is as follows. As seen in figure 5, the skewed nodal lines given by VIPASA in the case of shear do not coincide with the end edges. Forcing node lines to coincide with the end edges produces buckling loads that are always higher than those determined by VIPASA. When only one buckle forms along the panel

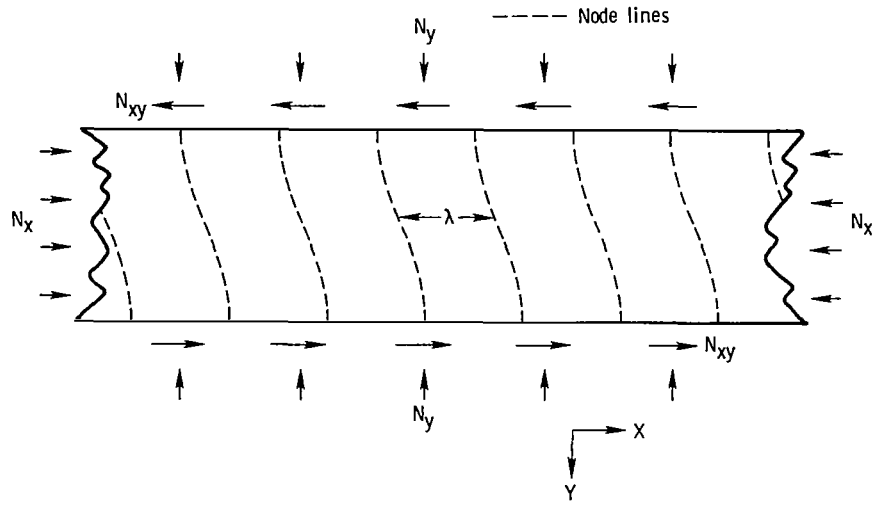

Figure 4.- Node lines for anisotropic plate elements and/or plate elements with shear loading.

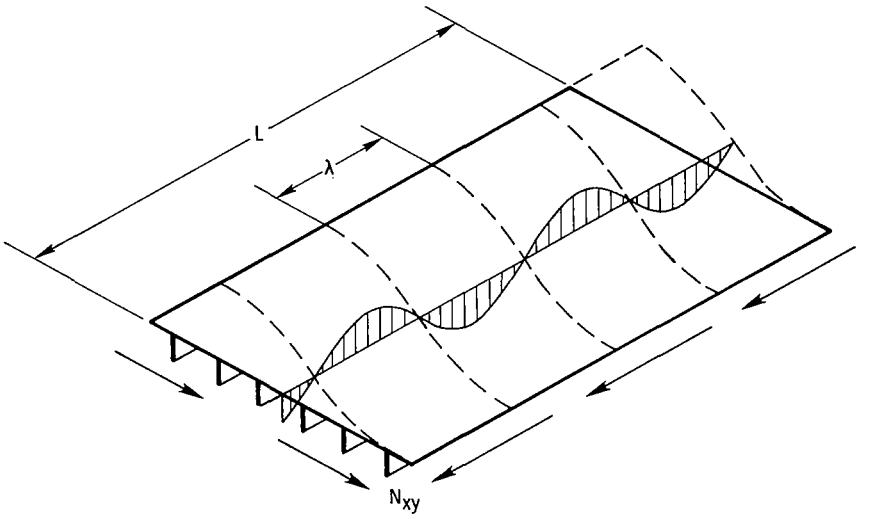

Figure 5.- Buckling of panel under shear loading. Mode shown is $\lambda = L/4$.

length, the effect of boundary conditions at the ends is much more important than when multiple buckles form along the length. For long-wavelength buckling modes, the buckling load for a panel satisfying the end boundary conditions can be more than twice the buckling load for a panel not satisfying the end boundary conditions. Such cases are illustrated in the examples discussed subsequently.

In summary, for stiffened panels composed of orthotropic plate elements with no shear loading, the VIPASA solution is exact in the sense that it is the exact solution of the plate equations satisfying the Kirchhoff-Love hypothesis. However, for stiffened panels having a shear loading, the VIPASA solution can be very conservative for the case $\lambda = L$.

Because VIPASA is overly conservative in the case of long-wavelength buckling if a shear load is present, another easily adaptable analysis procedure based on smeared orthotropic stiffnesses has been examined for the case $\lambda = L$. That attempt to get an improved solution is discussed in the following section.

Smeared Stiffener Solution

The objective of the analysis is to solve the shear buckling problem for the finite panel illustrated in figure 6. For buckling half-wavelength λ equal to panel length L, the mathematical model solved by VIPASA and the resulting node lines are similar to those illustrated in figure 7. The panel in figure 7 is infinitely long in the x-direction, but λ is finite.

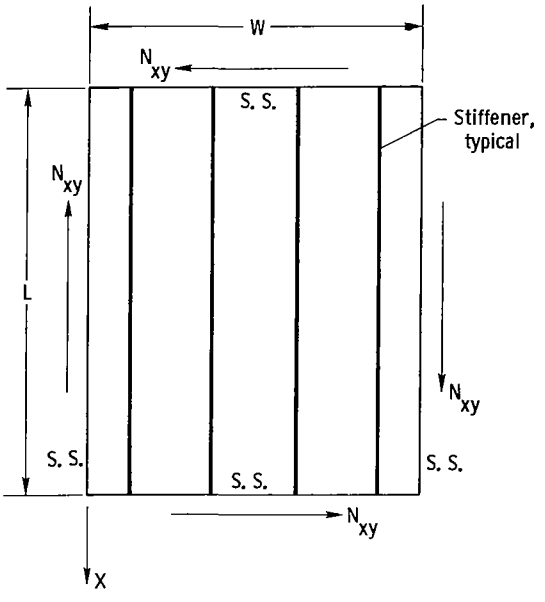

Figure 6.- Finite stiffened panel of length L and width W, simply supported on all four edges and subjected to shear load N_{xy}. S.S. designates simple support boundary conditions.

It is assumed that a better approximation to the solution for the finite panel would be obtained with the infinitely wide panel shown in figure 8. That assumption is based on the belief that, for this example, it is more important to satisfy boundary conditions along the edges perpendicular to the stiffeners than along the edges parallel to the stiffeners. There are two reasons for this belief. First, stiffeners tend to cause node lines to be nearly parallel to the stiffeners. This means that boundary conditions along edges parallel to the stiffeners

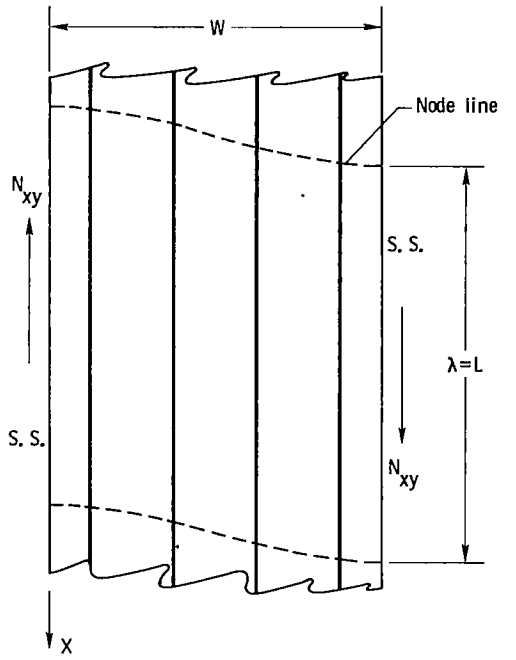

Figure 7.- Node lines given by VIPASA for shear buckling with $\lambda = L$. S.S. designates simple support boundary conditions.

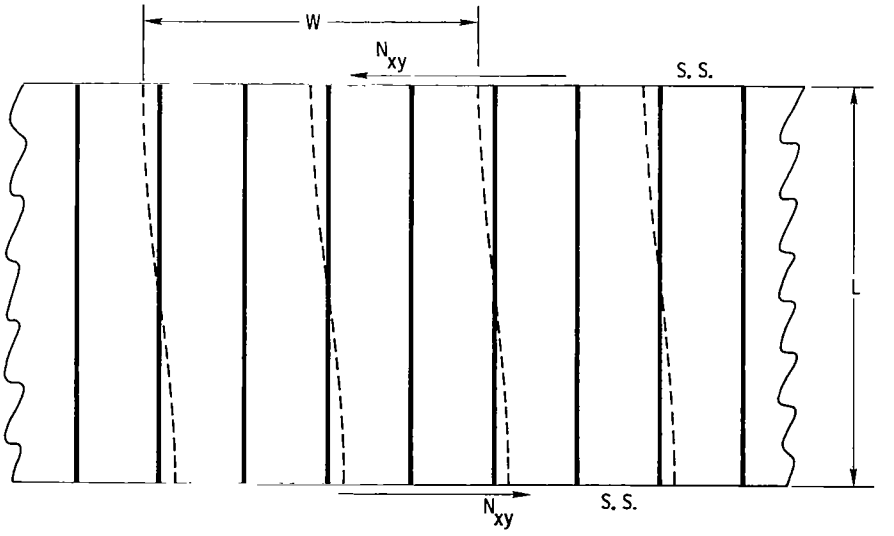

Figure 8.- Node lines for buckling of infinitely wide stiffened panel.

are more nearly satisfied automatically. Second, stiffeners tend to cause a buckle pattern having more half-waves transverse to the stiffeners than in the stiffener direction. Such a buckle pattern causes boundary conditions along edges parallel to the stiffeners to be relatively unimportant.

Unfortunately, the mathematical model illustrated in figure 8 cannot be analyzed with VIPASA because VIPASA requires that the panel be uniform in the direction of the infinite dimension. However, the mathematical model obtained by smearing the stiffnesses of the stiffened panel of figure 8 can be analyzed with VIPASA. That solution is referred to as the smeared stiffener solution. It is obtained by calculating orthotropic stiffnesses for the stiffened panel and interchanging the x and y loading and stiffnesses. Directions are changed because the x-direction is the infinite direction in VIPASA. The eigenvalue used is the lowest of the set for $\lambda = W, W/2, W/3, \ldots$, where W is the panel width.

The orthotropic stiffnesses involved in the smeared stiffener solution are the bending stiffnesses D_{11} and D_{22} and the twisting stiffness D_{33}. These stiffnesses are defined in the following differential equation for lateral deflection of an orthotropic plate with lateral loading q:

$$D_{11} \frac{\partial^2 w}{\partial x^4} + 4D_{33} \frac{\partial^4 w}{\partial x^2 \partial y^2} + D_{22} \frac{\partial^4 w}{\partial y^4} = q \tag{2}$$

The procedure used to calculate the orthotropic stiffnesses is described in reference 11.

The attempt to improve on the VIPASA solution for long-wavelength shear buckling is more involved than the discussion presented here. However, the basic feature - smeared stiffener solution - of that solution approach and the conclusions regarding its suitability are the same as those presented here. A more complete discussion of the procedure is presented in references 11 and 13. As is shown in the following examples, the smeared stiffener solution does, in some cases, provide an improved solution; however, the procedure should be used only with caution.

STIFFENED PANEL EXAMPLES

Seven stiffened panels were analyzed with PASCO and with the finite element structural analysis codes EAL (refs. 6 and 7) and STAGS (refs. 8 and 9). Results of these analyses are presented in this section. Four of the seven panels had blade stiffeners, one panel had hat stiffeners, one panel was a corrugated panel, and one panel had Z stiffeners. Four panels were modeled with a graphite-epoxy composite material; three were modeled with metal (aluminum). All panels were 30.0 in. (76.2 cm) square and had six equally spaced stiffeners. The loadings were combinations of longitudinal compression (N_x) and shear (N_{xy}). PASCO and EAL results are presented for each loading. STAGS results are presented only for the pure shear loadings and only for the first four examples - the blade-stiffened panels. The

VIPASA results provide an accurate check of the EAL model for pure longitudinal compression, and the STAGS results for the first four examples provide an independent check of the EAL results for pure shear. All standard VIPASA solutions (not the smeared stiffener solutions) include the effect of anisotropic bending stiffness terms for each plate element making up the panel cross section. The EAL and STAGS solutions also include anisotropic effects.

A schematic drawing showing the loading and overall dimensions for the seven example cases is shown in figure 9. The direction shown for N_{xy} in figure 9 is positive for EAL and STAGS (and for this report) and corresponds to a negative value of N_{xy} for PASCO. The positive orientation for the fiber orientation angle θ is also shown. For all panels and loadings, the stress analysis in PASCO (ref. 11) is used to distribute the applied loads over the panel cross section to obtain the prebuckling stress state. In particular, the N_x load is distributed by assuming uniform strain ϵ_x of the panel cross section with free transverse expansion of each plate element, so that N_y for each plate element is zero. PASCO, EAL, and STAGS buckling analyses all use the same prebuckling load distribution. A table containing the prebuckling load distribution for a typical loading is given for each example.

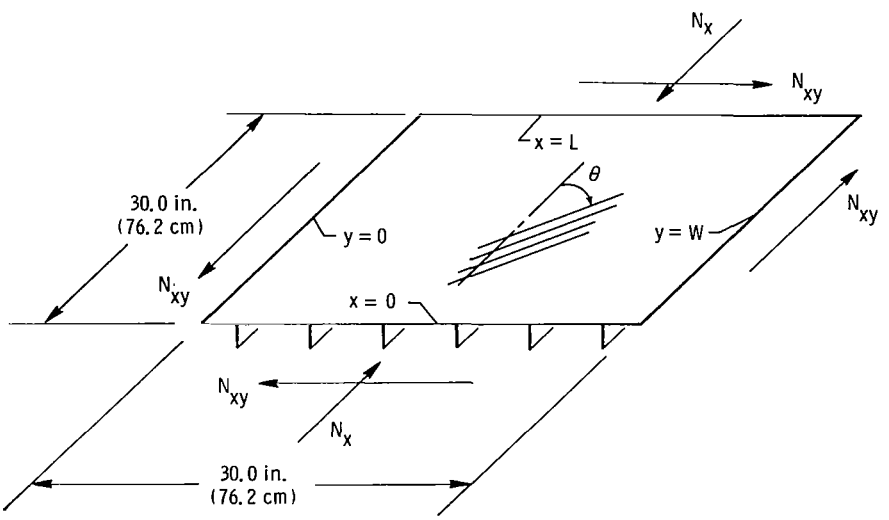

Figure 9.- Loading and dimensions for stiffened panel examples.

The goal is for buckling boundary conditions to be simple support on all four edges. These boundary conditions are applied to the stiffeners as well as to the skin. The simple support boundary conditions can be defined as follows:

At $x = 0, L;$ $\quad M_x = w = \delta N_x = \delta v = 0$

and at $y = 0, W;$ $\quad M_y = w = \delta N_y = \delta u = 0$

where δN_x, δv, δN_y, and δu represent changes in N_x, v, N_y, and u from the values in the prebuckling stress state. Buckling boundary conditions used by the analyses are as follows:

PASCO

At $x = 0, L$; boundary conditions cannot be prescribed. Simple support boundary conditions exist at the ends $x = 0$ and $x = L$ only for the pure compression case. See previous discussion in section entitled "VIPASA Buckling Analysis."

At $y = 0, W$; v and $\frac{\partial w}{\partial y}$ are unrestrained, and $u = w = 0$

EAL and STAGS

At $x = 0, L$; u and $\frac{\partial w}{\partial x}$ are unrestrained, and $v = w = \frac{\partial w}{\partial y} = 0$

At $y = 0, W$; v and $\frac{\partial w}{\partial y}$ are unrestrained, and $u = w = \frac{\partial w}{\partial x} = 0$

In each example, the solution denoted "VIPASA" is the standard VIPASA solution based on a detailed model of the panel cross section. The solution denoted "smeared stiffener solution" is also calculated with VIPASA, but the panel is modeled as an orthotropic plate.

The panel cross sections are treated as collections of lines with no offsets to account for thicknesses. (Offsets are available in PASCO, but were not used in order to allow direct comparison with other methods that cannot easily account for offsets.) The first example is discussed in greater detail than the other examples.

Example 1 - Composite Blade-Stiffened Panel

Panel description.- A repeating element of the composite blade-stiffened panel is shown in figure 10. Element widths are also shown. The wall construction for each plate element is given in table I. Only half the laminate is defined for each plate element because all laminates

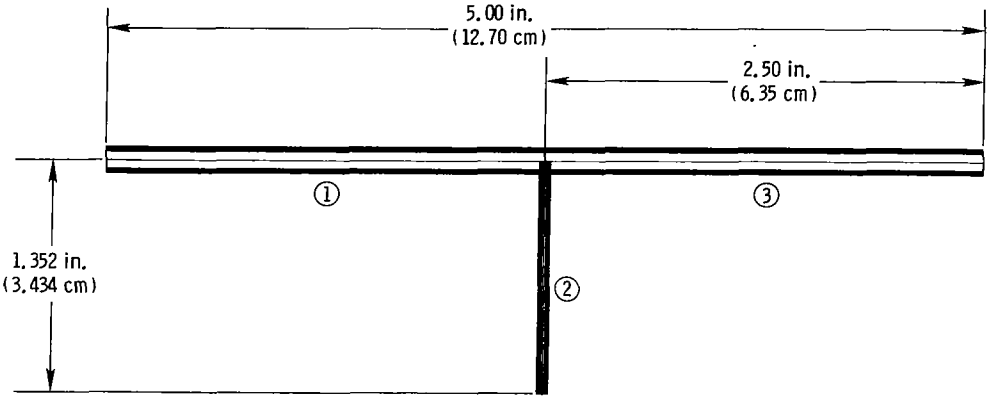

Figure 10.- Repeating element for example 1, composite blade-stiffened panel.

are symmetric. Plate element numbers are indicated by the circled numbers in figure 10. Fiber orientation angles are measured with respect to the X-axis, which is parallel to the stiffener direction.

Values of Young's moduli, shear modulus, and Poisson's ratio for the graphite-epoxy material used in the calculations for this example are given in table II.

Table III contains the prebuckling load distribution for the applied loading $N_x = N_{xy} = 1000$ lb/in. (175.1 kN/m). Since the prebuckling stress analysis treats longitudinal compression and shear separately, the prebuckling load distribution for other combinations of N_x and N_{xy} can be obtained by separately scaling the values of longitudinal compression and shear given in table III. The orthotropic stiffnesses used for the smeared stiffener solution are $D_{11} = 81\ 614$ lb-in. (9221.1 N-m), $D_{22} = 2893.1$ lb-in. (326.88 N-m), and $D_{33} = 1601.7$ lb-in. (180.97 N-m).

PASCO input.- Sample PASCO input for this example is shown in figure 11. The input for this and the other examples is in U.S. Customary Units. The loading is $N_x = 1000$, $N_{xy} = -1000$, which means that a solution is sought for the case $N_x = -N_{xy} = 1000$ lb/in. The

```
*****  EXAMPLE 1, COMPOSITE BLADE-STIFFENED PANEL  *****
$CONDAT
$
$PANEL
B=2.5, 1.352,  2.5,
T=.0055, .0055, .0495, .0055, .011,
THET=45, 0, 90, 45, 0,
KWALL(1,1)=1,-1,-1,1,2,3,
KWALL(1,2)=4,-4,-4,4,5,
IWALL=1,2,1,
HCARD=4,-4,2,90,0,
      2,121,4,
      4,5,1,3,-121,
ICARD=5,1,3,1,-909,0900,
      3,2,3,4,
      3,3,4,3,
      3,4,-909,0900,
NOBAY=6,
ICREP=6,
EL=30,
MINLAM=30,
NLAM=1,2,
SHEAR=1.,
IBC=1,
IP=2,
NX=1000.,
NXY=-1000.,
$
$MATER
E1=19.E6,   E2=1.89E6,   E12=.93E6,   ANU1=.38,   RHO=.0571,
$
```

Figure 11.- Sample PASCO input for example 1, composite blade-stiffened panel.

negative sign on N_{xy} causes the direction of N_{xy} in PASCO to agree with that shown in figure 9. The unknown in the PASCO eigenvalue analysis is a scalar factor which multiplies the load vector. ICARD input is included in order to get detailed plots of buckling mode shapes. The repeating element shown in figure 10 was generated with PASCO input.

EAL model.- The single finite element type used in the EAL model for this and the other examples is a four-node, quadrilateral, combined membrane and bending element. Both the membrane and bending stiffness matrices for the element are based on the assumed stress, hybrid formulation of Pian (refs. 6, 14, and 15). For this element, the geometric stiffness matrix that is required in the buckling analysis is based on a conventional displacement formulation that includes terms allowing inplane (u and v) as well as out-of-plane (w) displacements. The Pian membrane formulation allows a single element across the depth of a blade stiffener to represent accurately its overall inplane bending behavior. (Two elements were used to account for out-of-plane deformations.) The EAL designation for this element is E43.

The finite element grid chosen for the EAL model is shown in figure 12. Two elements are used along the depth of the blade, 4 elements are used between blades, and 36 elements are used along the length. Thus, a total of 1296 elements and 1369 nodes are present. A more refined model consisting of 3 elements along the depth of the blade, 4 elements between blades, and 48 elements along the length was used as a check for selected loadings. In all cases, the differences in the results for the two models were negligible. Also, since the PASCO solution is essentially exact for the pure compression case, PASCO results served as a guide when developing finite element models for EAL and STAGS.

It is recognized that the EAL model just described and the STAGS models described in the next section are more refined than models used in usual engineering calculations. However, since accuracy was an issue in this study, it was decided that benchmark calculations that differ from the exact solution by no more than approximately 1 percent were needed. Based on convergence studies and other comparisons, it is believed that the finite element calculations presented in this report meet this accuracy requirement.

As pointed out in a previous section, instead of solving the prebuckling stress problem with EAL and STAGS, the prebuckling load distribution is calculated with PASCO and is input to EAL and STAGS so that all three buckling analyses use a common prebuckling load distribution. Buckling boundary conditions used by EAL and STAGS were given on page 12. Additional details of the EAL input and analysis are given in the appendix.

STAGS model.- The single finite element type used in the STAGS model of this and the other examples is a six-node, triangular, combined membrane and bending element. The element is based on the Clough-Felippa triangle and has a displacement formulation. Midside nodes allow a single element across the depth of a blade stiffener to represent accurately its overall inplane bending behavior. The STAGS designation for this element is 422.

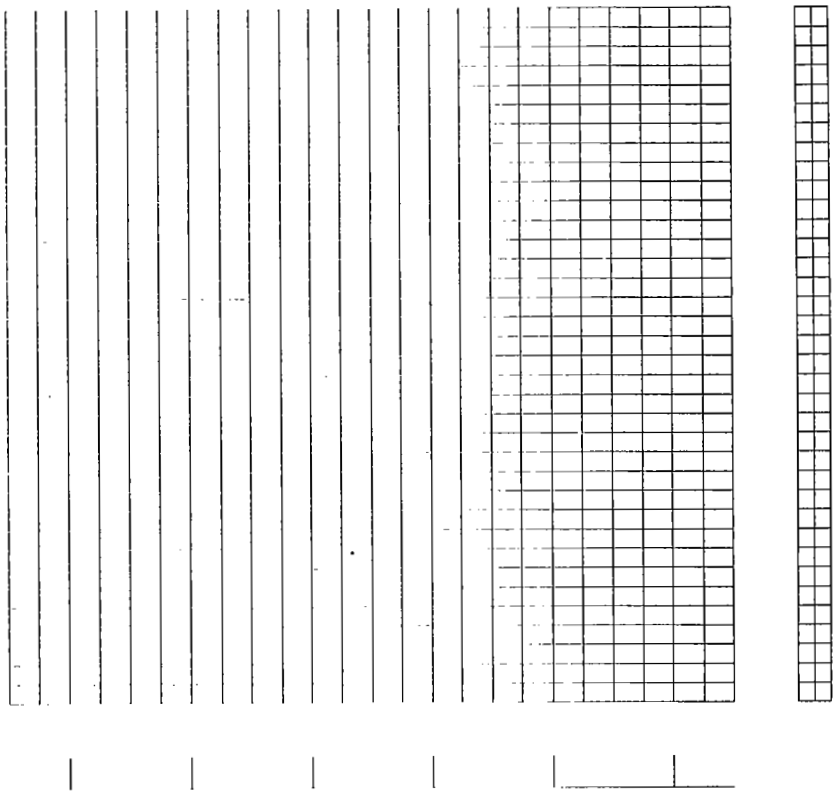

(a) Three views of model.

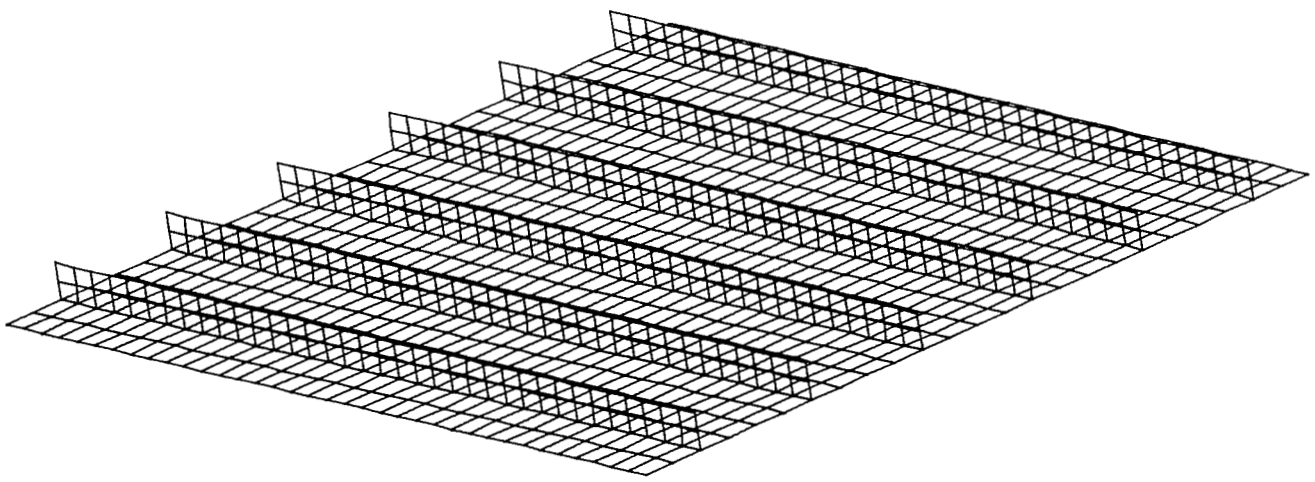

(b) Oblique view of model.

Figure 12.- EAL finite element model for example 1, composite blade-stiffened panel.

The finite element grid chosen for the STAGS model is shown in figure 13. The total number of triangular elements in the model is 2000. The total number of degrees of freedom in the model is 21 541. A more refined model containing four elements between blades was used as a check for selected loadings.

Results.- Buckling results obtained with PASCO, EAL, and STAGS are shown in figure 14. The curves indicate VIPASA and smeared stiffener solutions, and the symbols indicate EAL and STAGS solutions. The solid curve represents the VIPASA solution for buckling half-wavelength λ equal to L. The dotted line at the top of the figure represents the VIPASA solution for λ equal to L/2. Rather than presenting VIPASA solutions for only the lowest buckling load, VIPASA solutions are presented for the $\lambda = L$ mode and for the lowest mode other than the $\lambda = L$ mode. In this example, the additional mode is the $\lambda = L/2$ mode. The $\lambda = L$ mode is always shown because its conservatism in the presence of shear is a focus of this report.

The dashed curve in figure 14 represents the smeared stiffener solution and indicates solutions for the lowest buckling load of the set $\lambda = W, W/2, W/3, \ldots$, where W is the panel width. The slope change in the dashed curve that occurs at N_x equal to approximately 750 lb/in. (131 kN/m) indicates a change in mode shape for the smeared stiffener solution. For N_x less than 750 lb/in., the buckling half-wavelength transverse to the stiffeners is equal to 15.0 in. (38.1 cm), which is 3 times the stiffener spacing (5.0 in.). For N_x greater than 750 lb/in., the buckling half-wavelength transverse to the stiffeners is equal to 30 in., which is 6 times the stiffener spacing.

In this example, the smeared stiffener solution gives reasonably accurate estimates of the solution for all combinations of N_x and N_{xy}. For the pure shear loading, the smeared stiffener solution is about 5 percent lower than the EAL solution. For this same loading, the VIPASA solution for $\lambda = L$ is about 63 percent lower than the EAL solution. For the pure compression loading, the VIPASA solution for $\lambda = L$ and the EAL solution agree within 0.3 percent. For the pure shear loading, the STAGS and EAL solutions agree within 0.5 percent.

Detailed comparisons and benchmark calculations for six loadings are presented in table IV. In this table, the quantity denoted FACTOR is the buckling load in terms of a scale factor for the specified loading. For example, for the loading $N_x = 2000$ lb/in., $N_{xy} = 1000$ lb/in. ($N_x = 350.3$ kN/m, $N_{xy} = 175.1$ kN/m), the EAL solution of FACTOR = 0.4764 means that the buckling load is $N_x = 0.4764 \times 2000 = 952.8$ lb/in. (166.9 kN/m), $N_{xy} = 0.4764 \times 1000 = 476.4$ lb/in. (83.43 kN/m).

Also shown in table IV is an indication of the buckling mode shape determined by EAL for each loading. The designation of mode shapes as either symmetric (Sym) or antisymmetric (Anti) depends upon whether the buckling displacement w is symmetric or antisymmetric with respect to a point at the center of the panel.

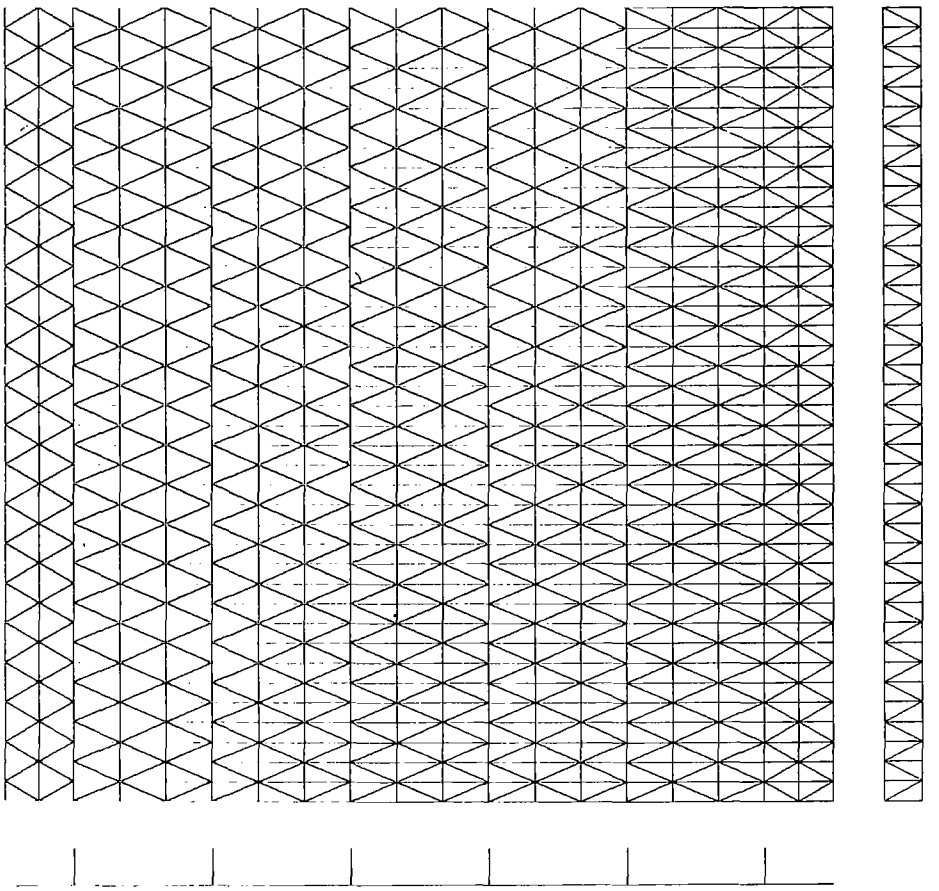

(a) Three views of model.

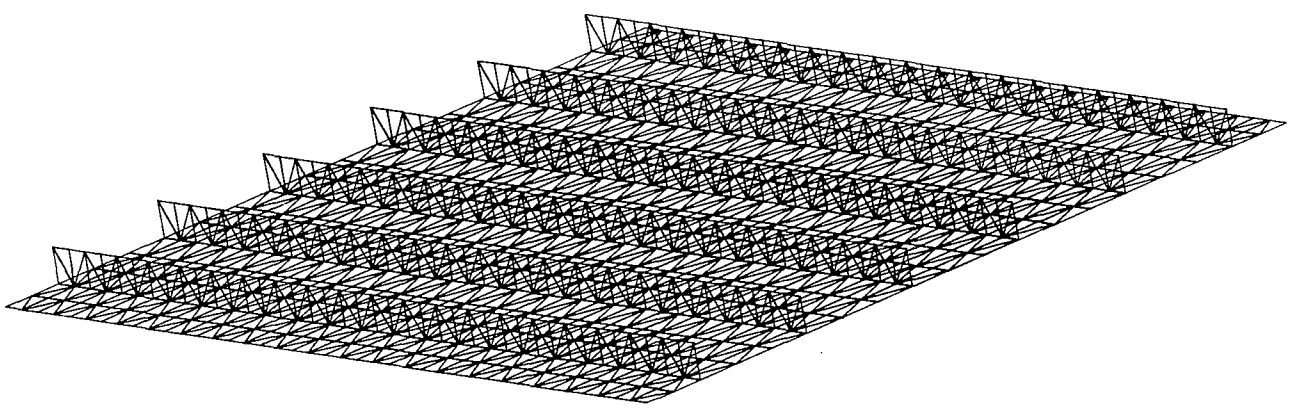

(b) Oblique view of model.

Figure 13.- STAGS finite element model for example 1, composite blade-stiffened panel.

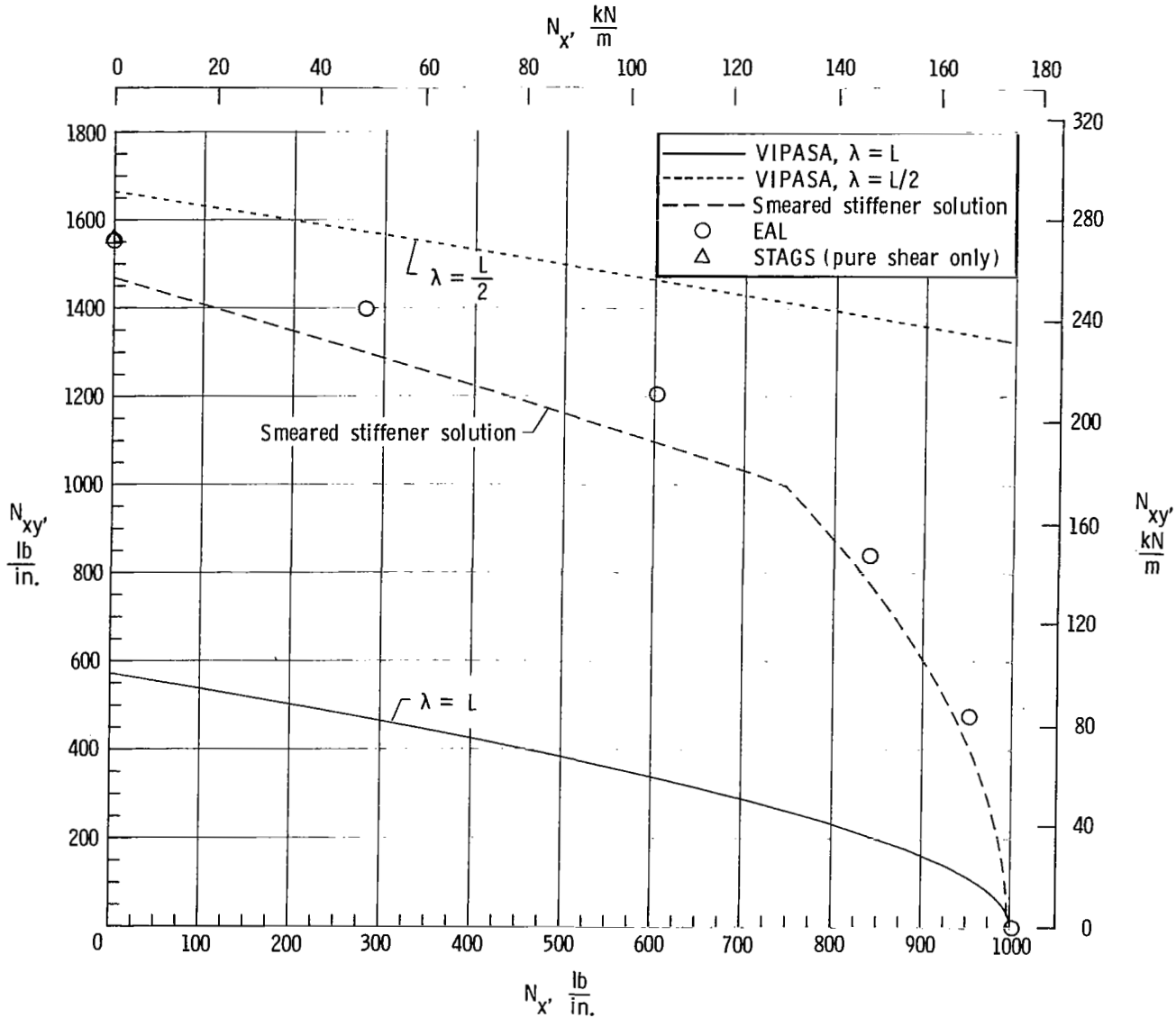

Figure 14.- Buckling load interaction for example 1, composite blade-stiffened panel.

Finally, the buckling mode shape obtained with EAL for the pure shear loading is shown in figure 15. The contour plot (fig. 15(b)) represents the buckling displacement w of the panel skin. This plot shows that the buckling half-wavelength transverse to the stiffeners is approximately equal to 3 times the stiffener spacing, as predicted by the smeared stiffener solution. This contour plot is an illustration of an antisymmetric buckling mode. The buckling mode shapes obtained with PASCO and EAL for pure compression are shown in figure 16.

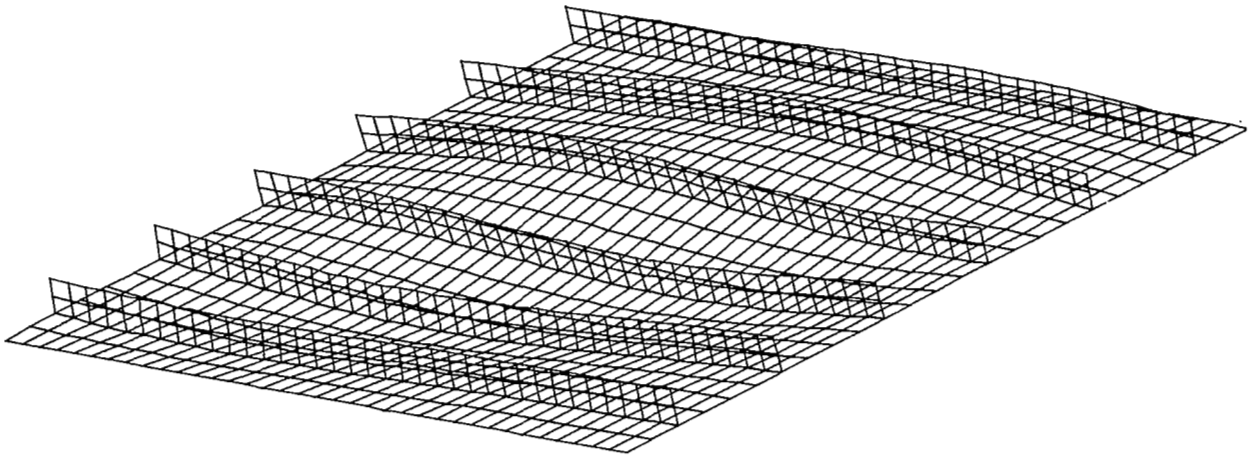

(a) Oblique view.

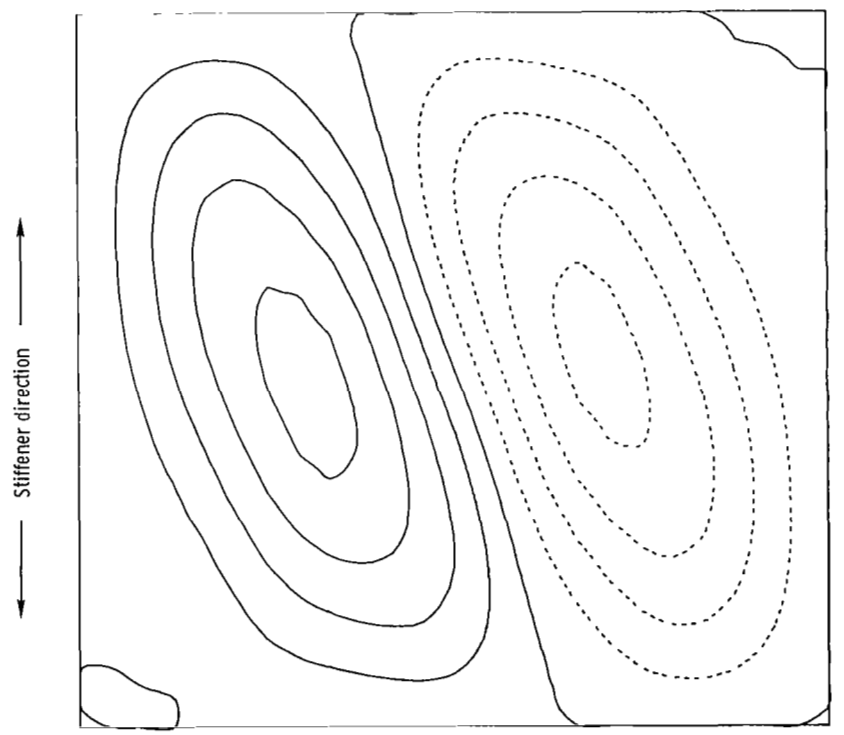

(b) Contour plot.

Figure 15.- Buckling mode shape for pure shear for example 1, composite blade-stiffened panel. Obtained with EAL.

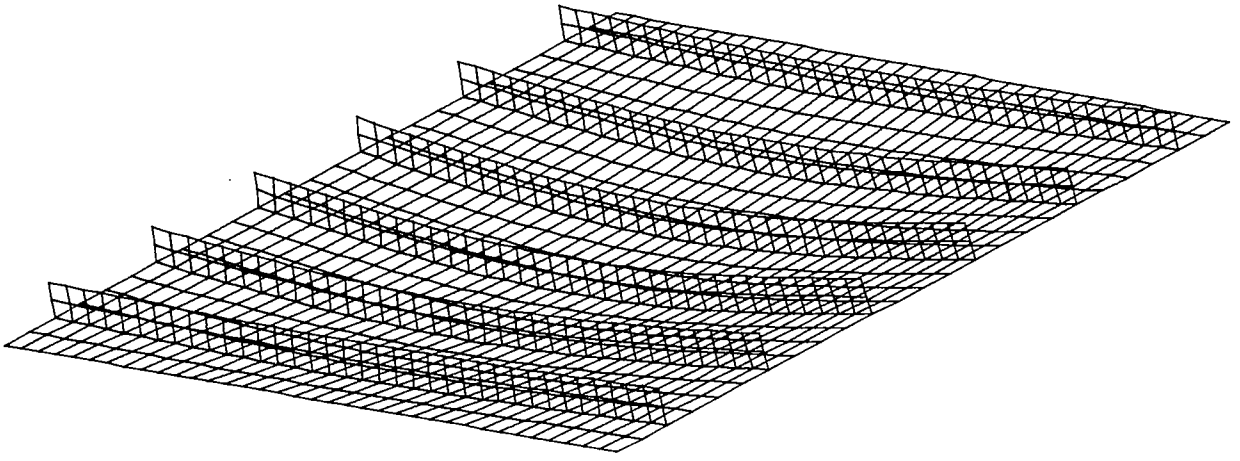

(a) Mode shape obtained with EAL.

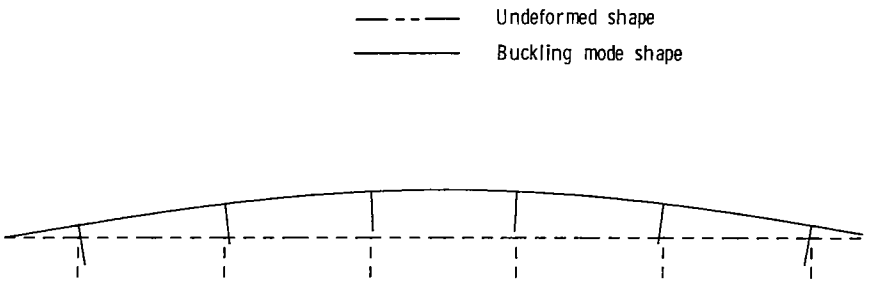

(b) Mode shape obtained with PASCO.

Figure 16.- Buckling mode shape for pure longitudinal compression for example 1, composite blade-stiffened panel.

TABLE I.- WALL CONSTRUCTION FOR EACH PLATE ELEMENT IN EXAMPLE 1, COMPOSITE BLADE-STIFFENED PANEL

[Only half the laminate is defined for each plate element because all laminates are symmetric]

Layer number, starting with outside layer	Thickness		Fiber orientation, θ, deg
	in.	cm	
Plate elements 1 and 3			
1	0.00550	0.01397	45
2	.00550	.01397	-45
3	.00550	.01397	-45
4	.00550	.01397	45
5	.00550	.01397	0
6	.04950	.12573	90
Plate element 2			
1	0.00550	0.01397	45
2	.00550	.01397	-45
3	.00550	.01397	-45
4	.00550	.01397	45
5	.01100	.02794	0

TABLE II.- PROPERTIES OF MATERIALS USED IN CALCULATIONS

Graphite-epoxy:

E_1, psi (GPa)	19×10^6	(131)
E_2, psi (GPa)	1.89×10^6	(13.0)
E_{12}, psi (GPa)	0.93×10^6	(6.41)
μ_1	0.38	
μ_2	0.0378	

Aluminum:

E, psi (GPa)	10.5×10^6	(72.4)
μ	0.32	

TABLE III.- PREBUCKLING LOAD DISTRIBUTION FOR EACH PLATE ELEMENT IN EXAMPLE 1, COMPOSITE BLADE-STIFFENED PANEL

[Applied loading is $N_x = N_{xy} = 1000.00$ lb/in. (175.13 kN/m)]

Load type	Internal load distribution			
	Plate elements 1 and 3		Plate element 2	
	lb/in.	kN/m	lb/in.	kN/m
N_x	811.35	142.09	697.67	122.18
N_{xy}	1000.00	175.13	0	0

TABLE IV.- VALUES OF FACTOR TO OBTAIN BUCKLING LOADS FOR EXAMPLE 1, COMPOSITE BLADE-STIFFENED PANEL

Applied load				Factor					EAL mode shape
N_x		N_{xy}		VIPASA		Smeared stiffener solution	EAL	STAGS	
lb/in.	kN/m	lb/in.	kN/m	$\lambda = L$	$\lambda = L/2$				
0	0	1000	175.1	0.5706	1.6600	1.4683	1.5525	1.5565	Anti
200	35.0	1000	175.1	.5339	1.5577	1.3098	1.3985		Anti
500	87.6	1000	175.1	.4851	1.4217	1.1222	1.2060		Anti
1000	175.1	1000	175.1	.4173	1.2332	.8222	.8397		Sym
2000	350.3	1000	175.1	.3194		.4690	.4764		Sym
1000	175.1	0	0	1.0005		.9970	1.0030		Sym

Example 2 - Metal Blade-Stiffened Panel

Panel description.- A repeating element of the metal blade-stiffened panel is shown in figure 17. Element widths and thicknesses are also shown. The material properties used in the calculations are $E = 10.5 \times 10^6$ psi (72.4 GPa), $\mu = 0.32$. The prebuckling load distribution is given in table V. The orthotropic stiffnesses used for the smeared stiffener solution are $D_{11} = 89\ 074$ lb-in., $D_{22} = 578.06$ lb-in., and $D_{33} = 314.61$ lb-in.

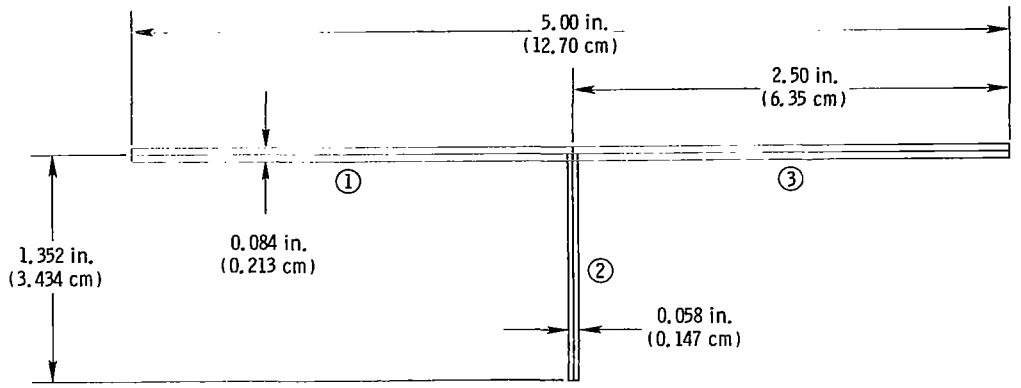

Figure 17.- Repeating element for example 2, metal blade-stiffened panel.

```
***** EXAMPLE 2, METAL BLADE-STIFFENED PANEL *****
$CONDAT
$
$PANEL
B=2.5, 1.352, 2.5,
T=.042, .029,
THET= 0, 0,
KWALL(1,1)=1,
KWALL(1,2)=2,
IWALL=1,2,1,
HCARD=4,-4,2,90,0,
      2,121,4,
      4,5,1,3,-121,
ICARD=5,1,3,1,-909,0900,
      3,2,3,4,
      3,3,4,3,
      3,4,-909,0900,
ICREP=6,
NOBAY=6,
SHEAR=1.,
EL=30,
MINLAM=30,
NLAM=1,2,3,
IBC=1,
IP=2,
NX=1000.,
NXY=-1000.,
$
$MATER
E1=10.5E6, E2=10.5E6, E12=3.9772727E6, ANU1=.32, RHO=.1,
$
```

Figure 18.- Sample PASCO input for example 2, metal blade-stiffened panel.

PASCO input.- Sample PASCO input for this example is shown in figure 18. As is the case with all examples in this report, ICARD input is included to get detailed plots of buckling mode shapes. The same numerical results are obtained when the modeling is carried out with HCARD input only. The repeating element shown in figure 17 was generated with PASCO input.

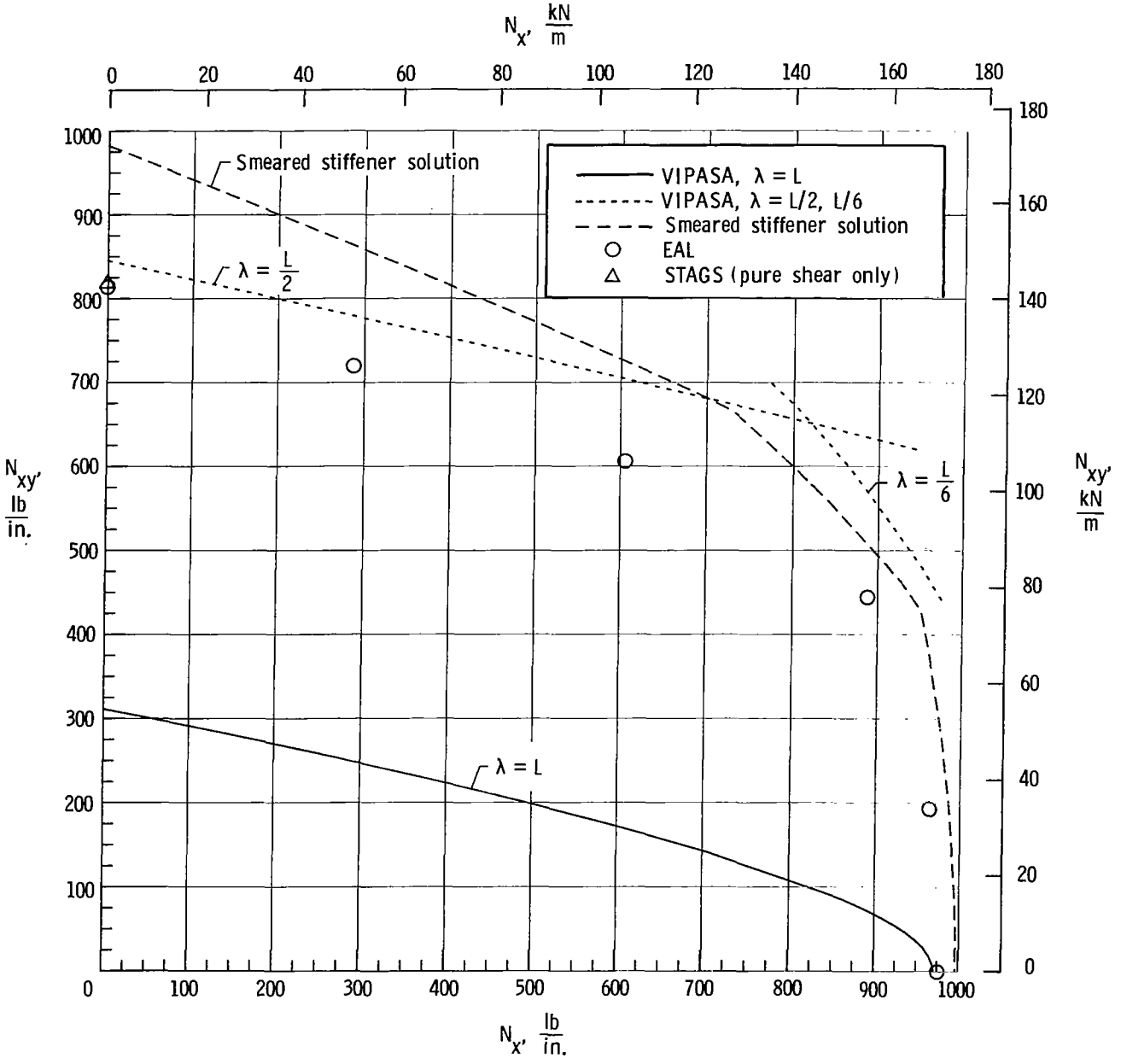

Figure 19.- Buckling load interaction for example 2, metal blade-stiffened panel.

EAL and STAGS models.- The same finite element type and grid pattern that are used in the EAL model of the first example are used in the EAL model for this example. Also, the finite element type and grid pattern used in the STAGS model of the first example are used in the STAGS model of this example.

Results.- Buckling results are shown in figure 19. The same general approach used for presenting the buckling results in the first example is used in this and subsequent examples. Curves indicate PASCO results, and symbols indicate EAL and STAGS results.

A portion of the standard VIPASA solution for $\lambda = L/2$, shown by the dotted line near the top of figure 19, is below the smeared stiffener solution. The slope changes in the smeared stiffener curve that occur at N_x equal to approximately 730 lb/in. (130 kN/m) and 950 lb/in. (166 kN/m) indicate a change in mode shape. For values of N_x less than about 730 lb/in., the buckling half-wavelength transverse to the stiffeners is equal to 10.0 in. (25.4 cm), which is twice the stiffener spacing. For values of N_x greater than 730 lb/in. but less than 950 lb/in., the buckling half-wavelength transverse to the stiffeners is 15.0 in. (38.1 cm), which is 3 times the stiffener spacing. For values of N_x greater than 950 lb/in., the buckling half-wavelength transverse to the stiffeners is 30.0 in. (76.2 cm), which is 6 times the stiffener spacing.

The curves representing the VIPASA results for $\lambda = L/2$ and the smeared stiffener solution are above the EAL and STAGS results. For the pure shear case, an examination of the EAL buckling mode shape (fig. 20) shows that the buckling mode is an overall mode ($\lambda = L$) rather than a $\lambda = L/2$ mode, which might have been assumed because the $\lambda = L/2$ solution is near the EAL and STAGS solutions. One possible factor contributing to the error in the smeared stiffener solution near $N_x = 0$ is that the buckling half-wavelength transverse to the stiffeners is too short to be a valid solution. A buckling half-wavelength that is at least 2.5 times the stiffener spacing would, in general, be necessary for a valid solution. However, even when such a buckle mode shape requirement is met, the smeared stiffener solution may not provide a good prediction of the buckling load. These results and results for subsequent examples show the danger of depending upon a smeared stiffener solution - even if the conservative assumption is made that the panel width is infinite rather than finite.

Detailed comparisons of solutions from PASCO, EAL, and STAGS for six loadings are presented in table VI. The buckling mode shape obtained with PASCO for the pure compression loading is shown in figure 21.

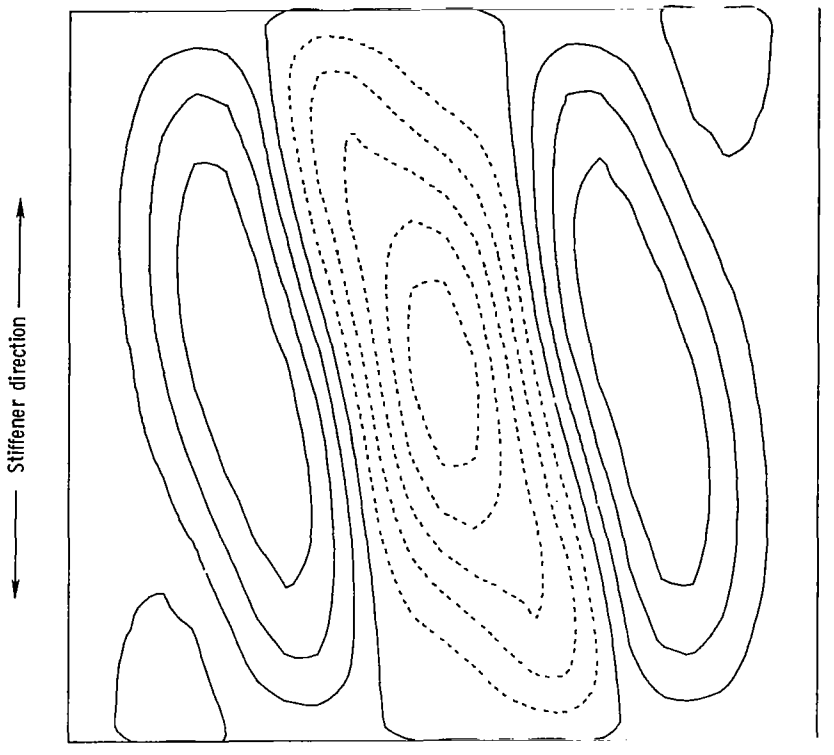

Figure 20.- Buckling mode shape for pure shear for example 2, metal blade-stiffened panel. Obtained with EAL.

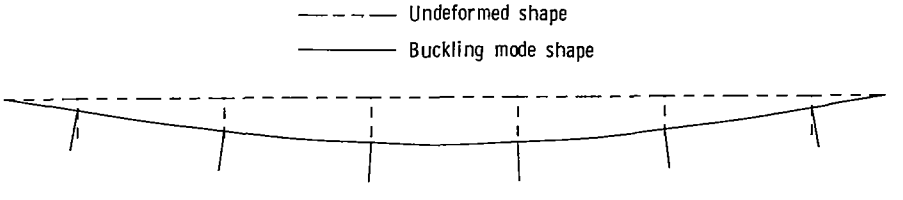

Figure 21.- Buckling mode shape for pure longitudinal compression for example 2, metal blade-stiffened panel. Obtained with PASCO.

TABLE V.- PREBUCKLING LOAD DISTRIBUTION FOR EACH PLATE ELEMENT IN EXAMPLE 2, METAL BLADE-STIFFENED PANEL

[Applied loading is $N_x = N_{xy} = 1000.00$ lb/in. (175.13 kN/m)]

Load type	Internal load distribution			
	Plate elements 1 and 3		Plate element 2	
	lb/in.	kN/m	lb/in.	kN/m
N_x	842.67	147.57	581.84	101.90
N_{xy}	1000.00	175.13	0	0

TABLE VI.- VALUES OF FACTOR TO OBTAIN BUCKLING LOADS FOR EXAMPLE 2, METAL BLADE-STIFFENED PANEL

Applied load				Factor					EAL mode shape
N_x		N_{xy}		VIPASA		Smeared stiffener solution	EAL	STAGS	
lb/in.	kN/m	lb/in.	kN/m	$\lambda = L$	$\lambda = L/2$				
0	0	1000	175.1	0.3118	0.8450	0.9823	0.8138	0.8179	Sym
400	70.0	1000	175.1	.2877	.7742	.8423	.7195		Sym
1000	175.1	1000	175.1	.2568	.6849	.6879	.6061		Sym
2000	350.3	1000	175.1	.2159		.4637	.4444		Anti
5000	875.6	1000	175.1	.1413		.1975	.1929		Sym
1000	175.1	0	0	.9710		.9969	.9759		Sym

Example 3 - Heavily Loaded, Composite Blade-Stiffened Panel

Panel description.- A repeating element of the heavily loaded, composite blade-stiffened panel is shown in figure 22. The wall construction for each plate element is given in table VII. Only half the laminate is defined for each plate element because all laminates are symmetric. Plate element numbers are indicated by the circled numbers in figure 22.

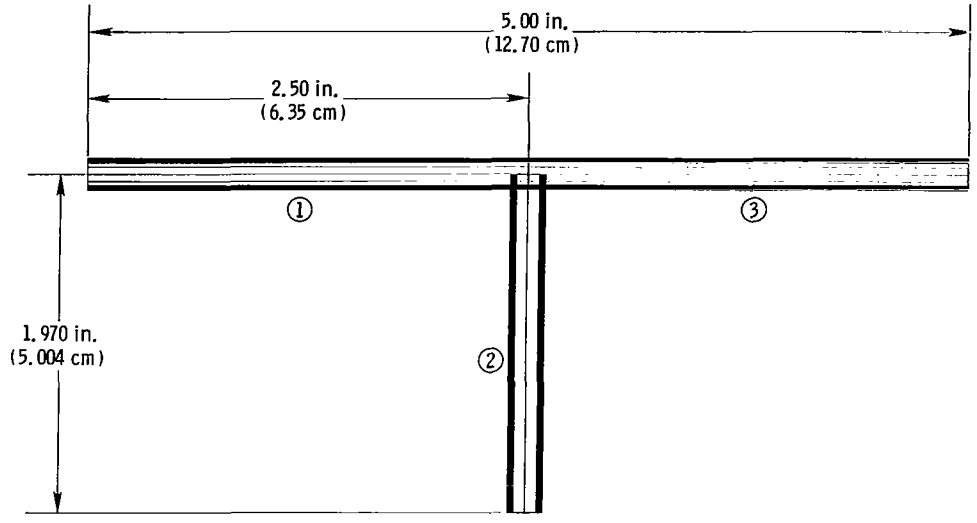

Figure 22.- Repeating element for example 3, heavily loaded, composite blade-stiffened panel.

```
*****  EXAMPLE 3, COMPOSITE BLADE-STIFFENED PANEL, HEAVILY LOADED  *****
 $CONDAT
 $
 $PANEL
 GRANGE=10,
 B=2.5, 1.97, 2.5,
 T=.00637, .0249, .0416, .00823, .0675,
 THET=45, 0, 90, 45, 0,
 KWALL(1,1)=1,-1,-1,1,2,3,
 KWALL(1,2)=4,-4,-4,4,5,
 IWALL=1,2,1,
 HCARD=4,-4,2,90,0,
       2,121,4,
       4,5,1,3,-121,
 ICARD=5,1,3,1,-909,0900,
       3,2,3,4,
       3,3,4,3,
       3,4,-909,0900,
 NOBAY=6,
 ICREP=6,
 EL=30,
 MINLAM=30,
 NLAM=1,2,3,
 SHEAR=1.,
 IBC=1,
 IP=2,
 NX=1000.,
 NXY=-1000.,
 $
 $MATER
 E1=19.E6,   E2=1.89E6,  E12=.93E6,  ANU1=.38,  RHO=.0571,
 $
```

Figure 23.- Sample PASCO input for example 3, heavily loaded, composite blade-stiffened panel.

Values for material properties are the same as those used in example 1 and are given in table II. The prebuckling load distribution is given in table VIII, and the orthotropic stiffnesses are D_{11} = 958 850 lb-in., D_{22} = 3339.4 lb-in., and D_{33} = 4066.7 lb-in.

PASCO input and EAL and STAGS models.- Sample PASCO input for this example is shown in figure 23. The same finite element types and grid patterns used in the EAL and STAGS models of the first example are used in this example.

Results.- Buckling solutions for example 3 are shown in figure 24. The solid curve indicates the VIPASA solution for $\lambda = L$. The dotted curves indicate VIPASA solutions for

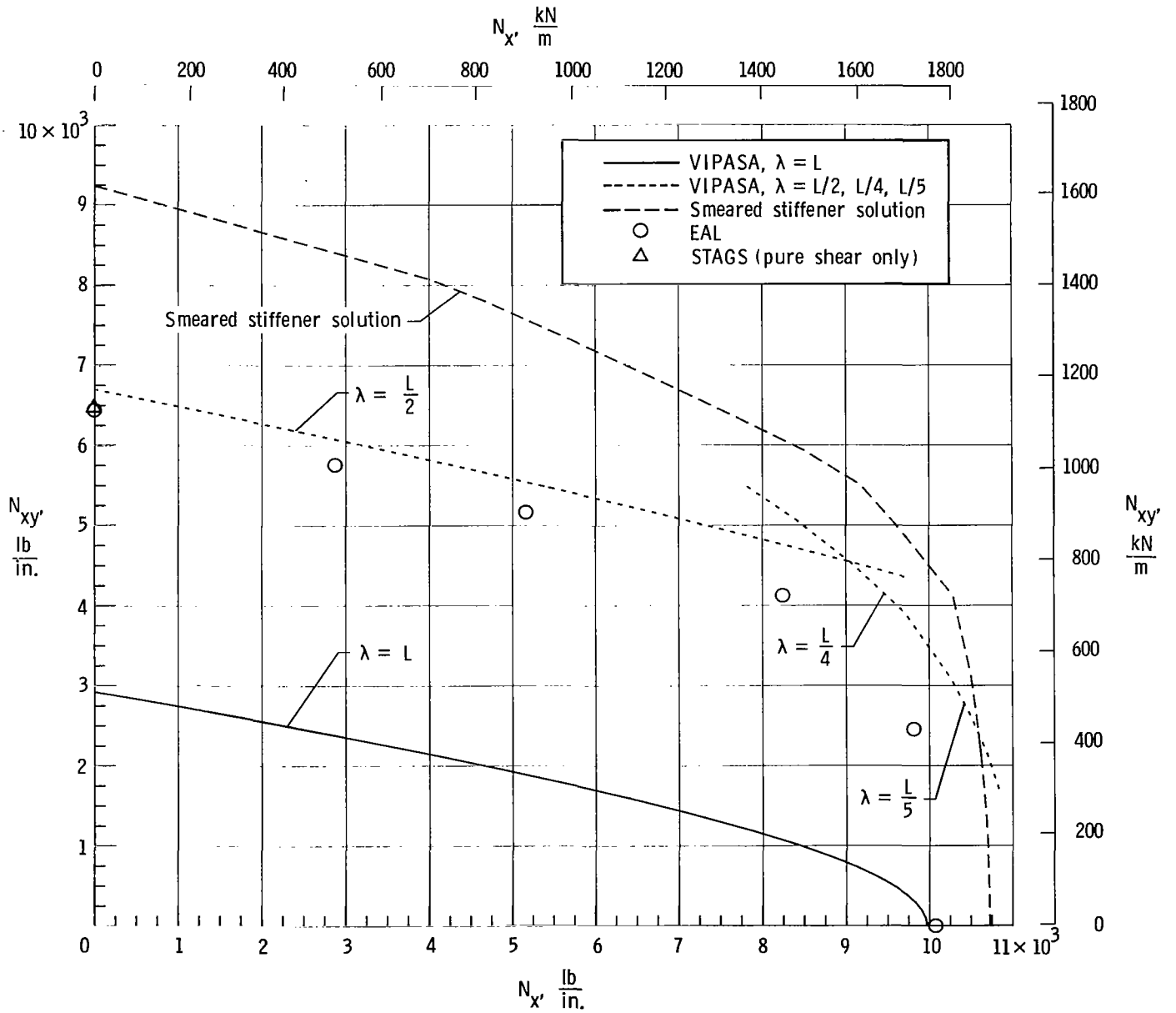

Figure 24.- Buckling load interaction for example 3, heavily loaded, composite blade-stiffened panel.

$\lambda = L/2$, $L/4$, and $L/5$. The dashed curve represents the smeared stiffener solution. As in the first example, the slope changes in the dashed curve indicate changes in mode shape. These changes in slope occur at N_x equal to approximately 4000 lb/in. (700 kN/m), 9200 lb/in. (1610 kN/m), and 10 300 lb/in. (1800 kN/m). For N_x less than about 4000 lb/in., the buckling half-wavelength transverse to the stiffeners is 1.5 times the stiffener spacing. For N_x greater than about 4000 lb/in. but less than about 9200 lb/in., the buckling half-wavelength transverse to the stiffeners is 2 times the stiffener spacing. For N_x greater than about 9200 lb/in. but less than about 10 300 lb/in., the buckling half-wavelength transverse to the stiffeners is 3 times the stiffener spacing.

The curves representing the VIPASA results for $\lambda = L/2$, $L/4$, and $L/5$ and the smeared stiffener solution are all above the EAL and STAGS results. As in example 2, the buckling mode for the EAL analysis with a pure shear loading is an overall mode - not a $\lambda = L/2$ mode.

Detailed comparisons of solutions from PASCO, EAL, and STAGS for six loadings are presented in table IX. The buckling mode shape obtained with EAL for the pure shear loading is shown in figure 25. The buckling mode shape obtained with PASCO for the pure compression loading is shown in figure 26.

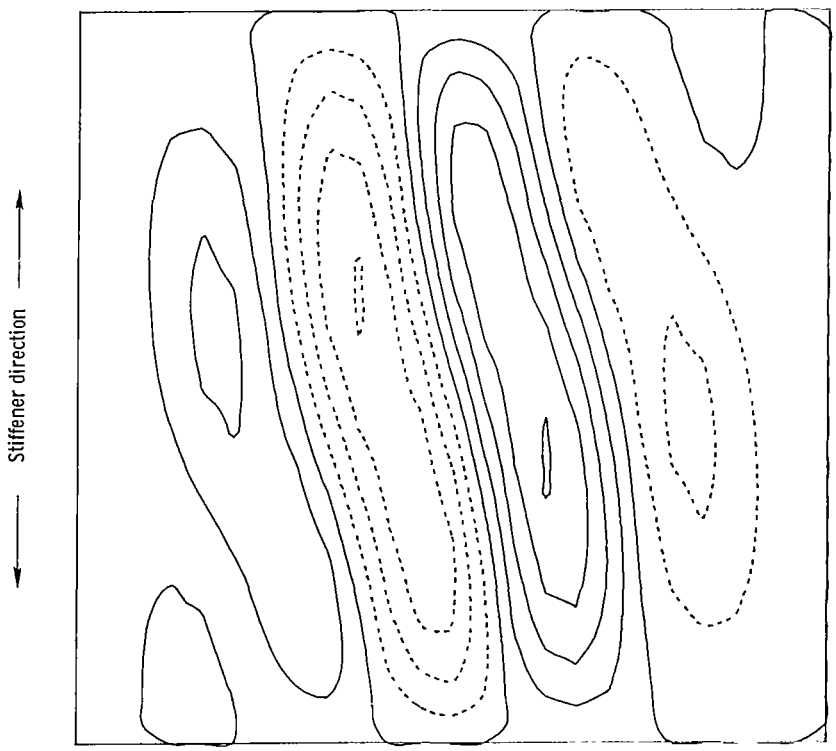

Figure 25.- Buckling mode shape for pure shear for example 3, heavily loaded, composite blade-stiffened panel. Obtained with EAL.

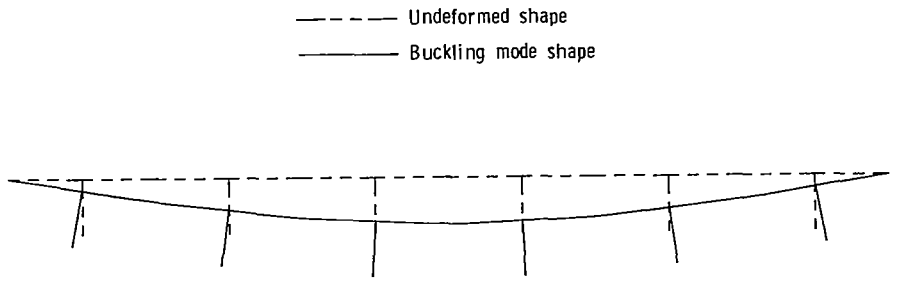

Figure 26.- Buckling mode shape for pure longitudinal compression for example 3, heavily loaded, composite blade-stiffened panel. Obtained with PASCO.

TABLE VII.- WALL CONSTRUCTION FOR EACH PLATE ELEMENT IN EXAMPLE 3, HEAVILY LOADED, COMPOSITE BLADE-STIFFENED PANEL

[Only half the laminate is defined for each plate element because all laminates are symmetric]

Layer number, starting with outside layer	Thickness		Fiber orientation, θ, deg
	in.	cm	
Plate elements 1 and 3			
1	0.00637	0.01618	45
2	.00637	.01618	-45
3	.00637	.01618	-45
4	.00637	.01618	45
5	.02490	.06325	0
6	.04160	.10566	90
Plate element 2			
1	0.00823	0.02090	45
2	.00823	.02090	-45
3	.00823	.02090	-45
4	.00823	.02090	45
5	.06750	.17145	0

TABLE VIII.- PREBUCKLING LOAD DISTRIBUTION FOR EACH PLATE ELEMENT IN EXAMPLE 3, HEAVILY LOADED, COMPOSITE BLADE-STIFFENED PANEL

[Applied loading is $N_x = N_{xy} = 1000.00$ lb/in. (175.13 kN/m)]

Load type	Internal load distribution			
	Plate elements 1 and 3		Plate element 2	
	lb/in.	kN/m	lb/in.	kN/m
N_x	559.71	98.02	1117.50	195.70
N_{xy}	1000.00	175.13	0	0

TABLE IX.- VALUES OF BUCKLING LOADS FOR EXAMPLE 3, HEAVILY LOADED, COMPOSITE BLADE-STIFFENED PANEL

Applied load				Factor					EAL mode shape
N_x		N_{xy}		VIPASA		Smeared stiffener solution	EAL	STAGS	
lb/in.	kN/m	lb/in.	kN/m	$\lambda = L$	$\lambda = L/2$				
0	0	1000	175.1	2.9179	6.6855	9.2435	6.4424	6.470	Anti
500	87.6	1000	175.1	2.6703	6.0262	8.0628	5.753		Anti
1000	175.1	1000	175.1	2.4540	5.4549	6.7945	5.1630		Anti
2000	350.3	1000	175.1	2.0972	4.5289	4.8627	4.124		Sym
4000	700.5	1000	175.1	1.5949		2.6424	2.4543		Sym
1000	175.1	0	0	9.9724		10.7300	10.076		Sym

Example 4 - Metal Blade-Stiffened Panel With Thin Skin

Panel description.- A repeating element of the metal blade-stiffened panel with thin skin is shown in figure 27. Element widths and thicknesses are also shown. The material properties used in the calculations are $E = 10.5 \times 10^6$ psi (72.4 GPa), $\mu = 0.32$. Except for the thickness of the skin, this panel is the same as that used in example 2. The prebuckling load distribution is given in table X. The orthotropic stiffnesses are $D_{11} = 82\ 490$ lb-in., $D_{22} = 121.92$ lb-in., and $D_{33} = 86.641$ lb-in.

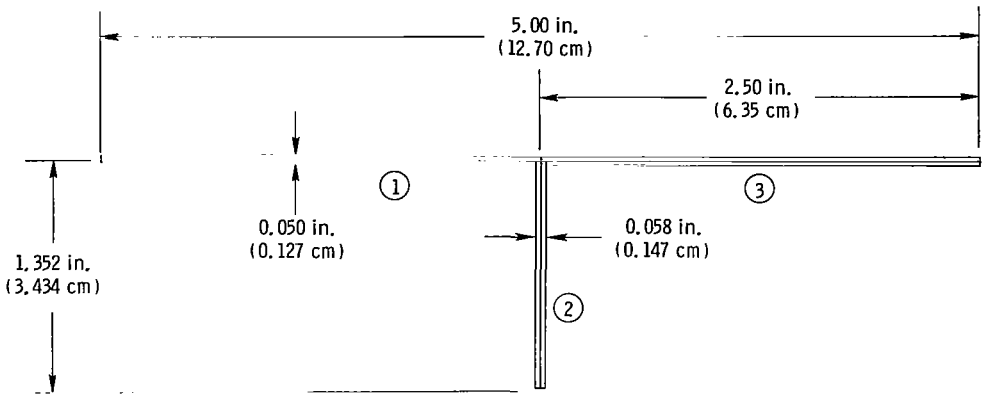

Figure 27.- Repeating element for example 4, metal blade-stiffened panel with thin skin.

PASCO input and EAL and STAGS models.- PASCO input for this example is the same as that given in figure 18 except that thickness T(1) = 0.025. The same finite element types and grid patterns used in the EAL and STAGS models of the first example are used in this example.

Results.- Buckling results obtained with PASCO, EAL, and STAGS are shown in figure 28. The same general approach used for presenting buckling data in previous examples is used in this example. Because the skin is thinner for this example than for example 2, the dominant buckling mode is a local mode rather than an overall mode.

The solid curve represents the standard VIPASA solution for $\lambda = L$. The dotted curve represents the standard VIPASA solutions for $\lambda = L/5$ and $\lambda = L/6$. The dashed curve represents the smeared stiffener solution. For the pure shear loading, the smeared stiffener solution has a buckling half-wavelength transverse to the stiffeners that is 1.2 times the stiffener spacing. That buckling half-wavelength is much too short to provide a valid solution.

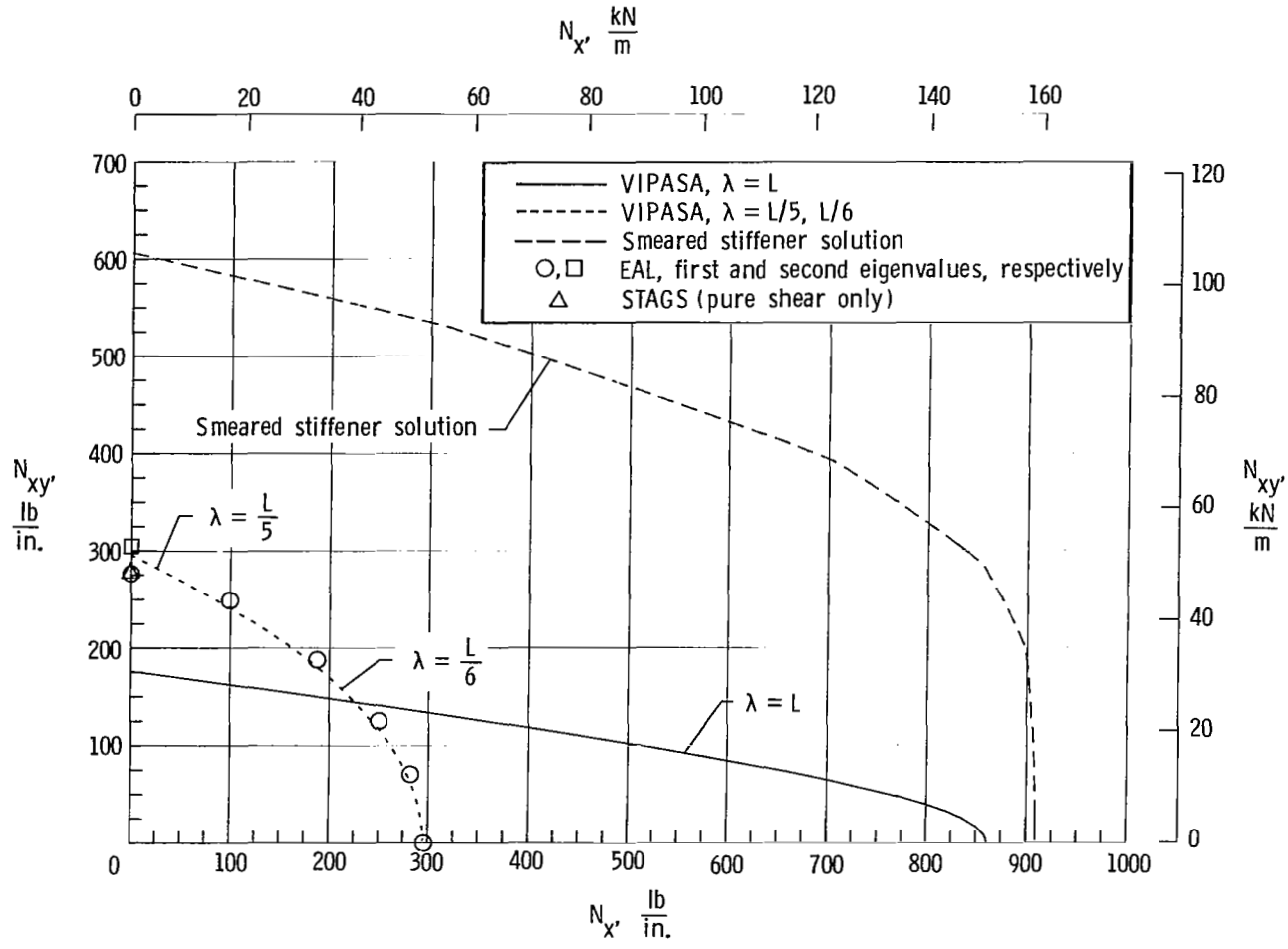

Figure 28.- Buckling load interaction for example 4, metal blade-stiffened panel with thin skin.

The EAL results are very near the VIPASA short-wavelength results indicated by the dotted curve. Except for the pure shear case, the EAL results are slightly higher than the VIPASA short-wavelength results. For the pure shear case, the lowest eigenvalue for both EAL and STAGS appears to be primarily an overall mode (in the stiffener direction) rather than a local mode. The mode shape for this first eigenvalue is shown in figure 29. The second eigenvalue obtained from EAL for a pure shear loading is a local mode and is shown in figure 30.

Detailed comparisons of solutions from PASCO, EAL, and STAGS for six loadings are presented in table XI. The buckling mode shapes obtained with EAL and PASCO for the pure compression loading are shown in figure 31.

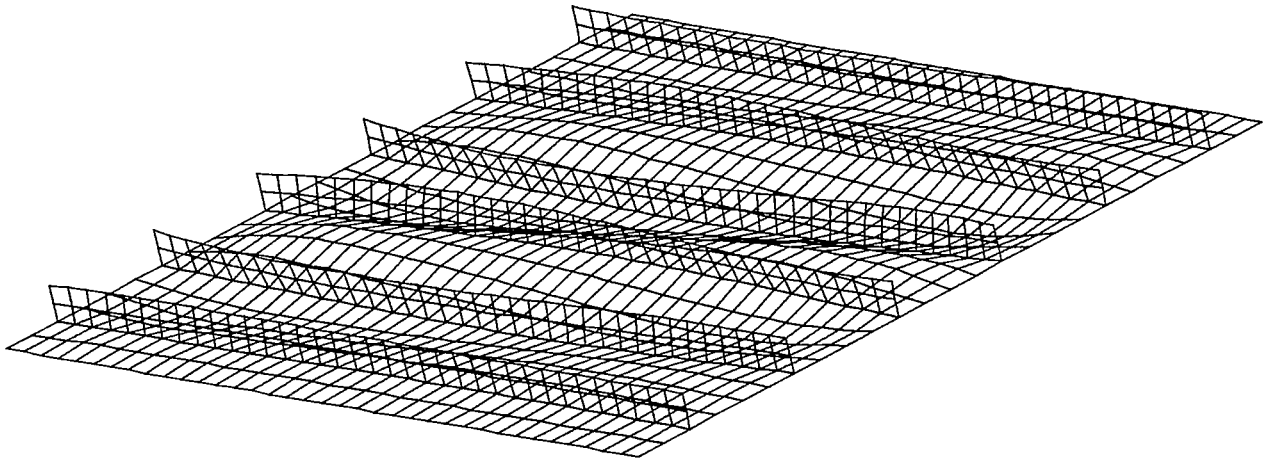

(a) Oblique view.

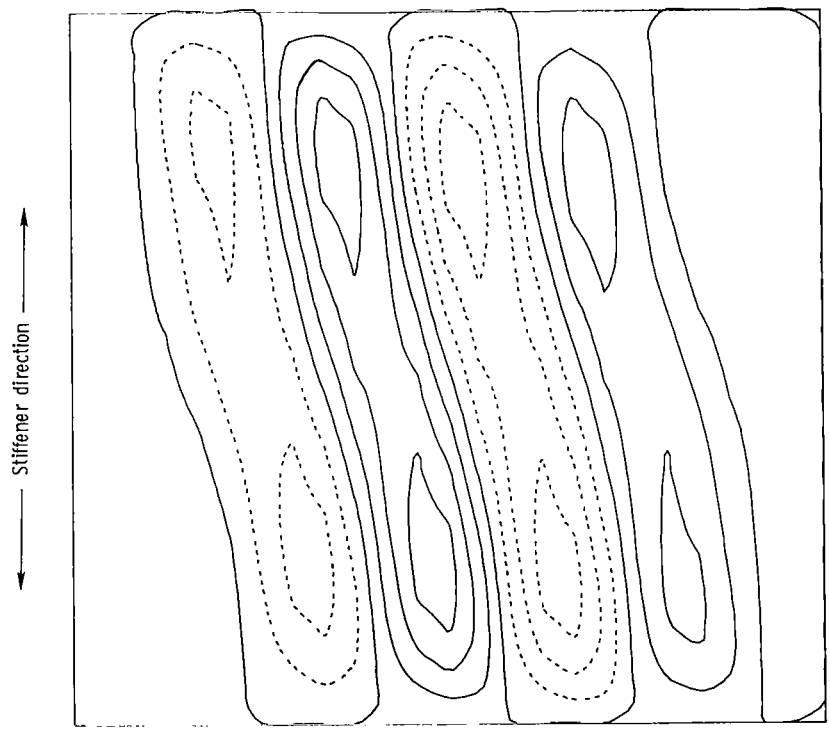

(b) Contour plot.

Figure 29.- Buckling mode shape for first eigenvalue, pure shear, for example 4, metal blade-stiffened panel with thin skin. Obtained with EAL.

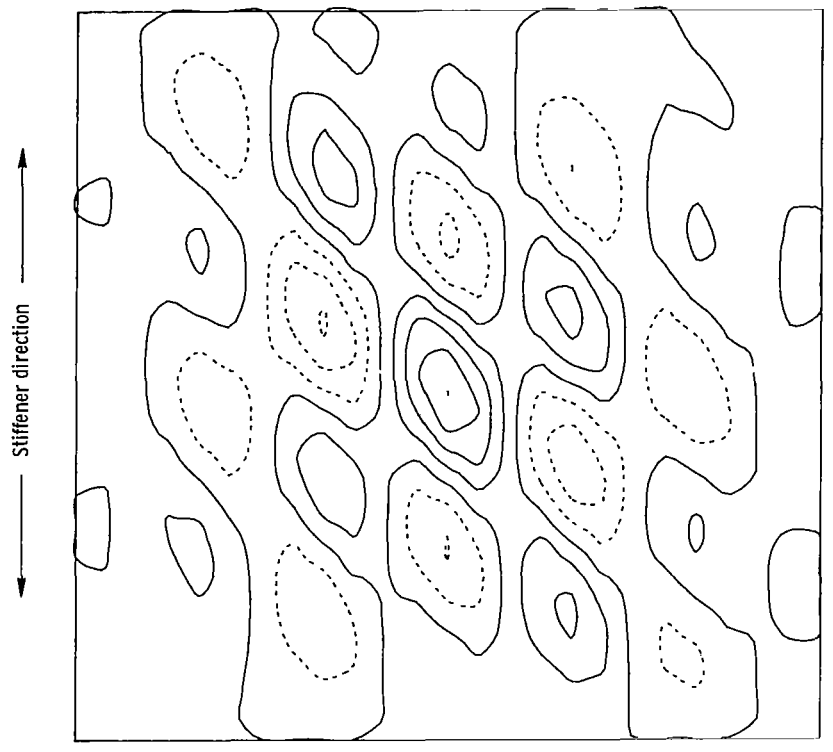

Figure 30.- Buckling mode shape for second eigenvalue, pure shear, for example 4, metal blade-stiffened panel with thin skin. Obtained with EAL.

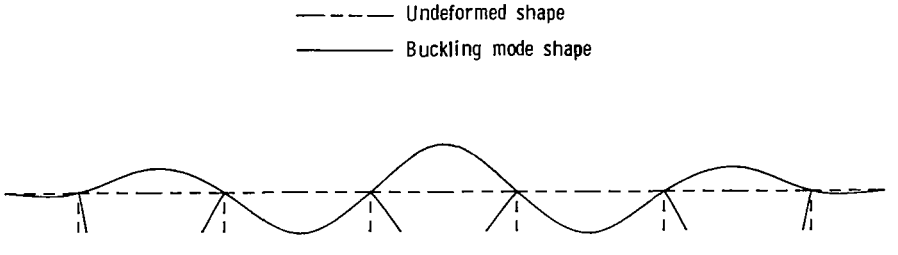

(a) Mode shape obtained with PASCO.

Figure 31.- Buckling mode shape for pure longitudinal compression for example 4, metal blade-stiffened panel with thin skin.

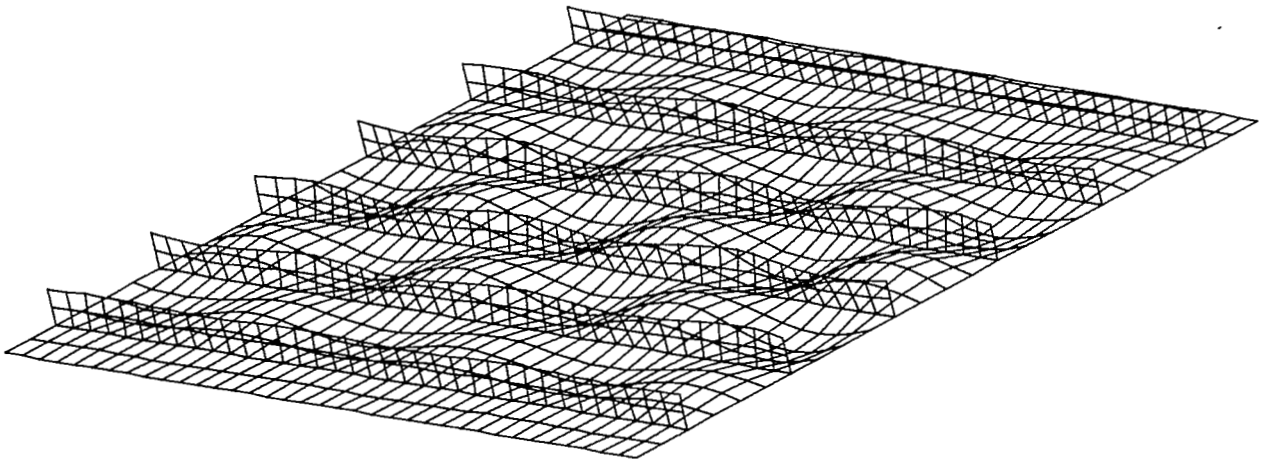

(b) Oblique view of mode shape obtained with EAL.

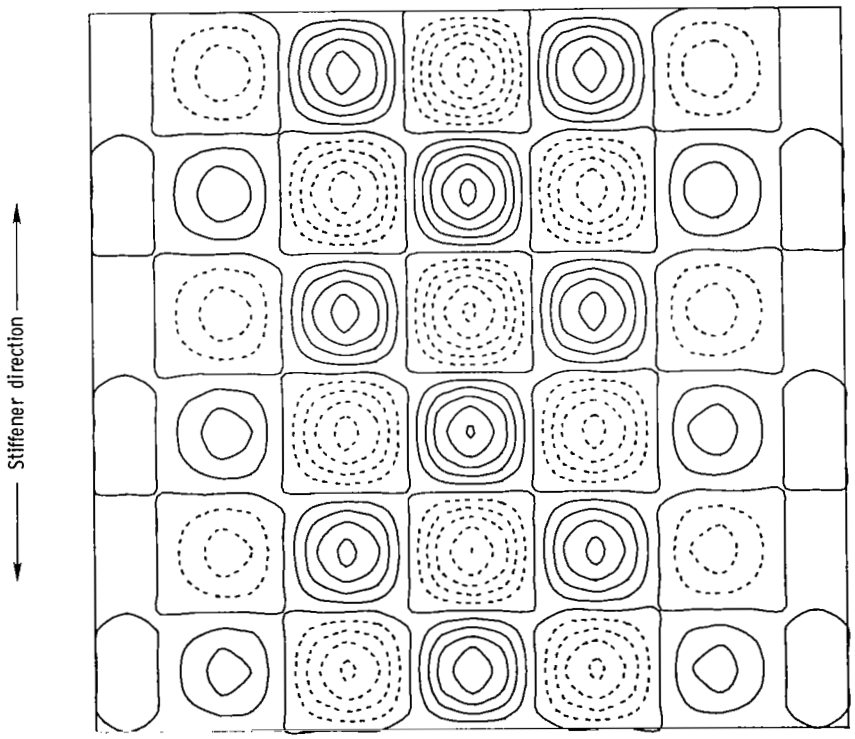

(c) Contour plot of mode shape obtained with EAL.

Figure 31.- Concluded.

Because the first eigenvalue for pure compression and the second eigenvalue for pure shear are local modes, a simplified local buckling analysis was also performed on this panel. For the pure compression case, local buckling of the skin can be estimated by assuming that the skin between stiffeners is a narrow, simply supported strip. The buckling load of the skin is given by

$$N_{x_{cr}} = 4 \frac{\pi^2 D}{b^2} \tag{3}$$

where D is the plate bending stiffness (121.9 lb-in.) and b is the plate width (5 in.). The result is $N_{x_{cr}} = 192$ lb/in. According to PASCO, when the panel buckles, the load in the skin is 225 lb/in. In this case, the stiffeners are providing rotational support to the skin. This can be shown by calculating the buckling load of the stiffeners with a formula (ref. 16, pp. 360-362) that is similar to equation (3). That formula is

$$N_{x_{cr}} = 0.5 \frac{\pi^2 D}{b^2} \tag{4}$$

where D is 190.2 lb-in. and b is 1.352 in. The result is $N_{x_{cr}} = 513$ lb/in. According to PASCO, when the panel buckles, the load in the stiffeners is 261 lb/in. The skin is destabilizing the stiffeners, or, conversely, the stiffeners are stabilizing the skin. Further discussion of the concept of rotational restraint at the juncture of plate elements is presented in reference 17. (See, particularly, fig. 14 of ref. 17.)

For the pure shear case, local buckling of the skin can be approximated by the formula (ref. 16, p. 383)

$$N_{xy_{cr}} = 5.35 \frac{\pi^2 D}{b^2} \tag{5}$$

where D and b are given following equation (3). The result is $N_{xy_{cr}} = 257$ lb/in. According to PASCO and EAL, the shear load in the skin when the panel buckles in a local mode is about 300 lb/in. As in the pure compression case, the stiffeners are providing rotational support to the skin.

TABLE X.- PREBUCKLING LOAD DISTRIBUTION FOR EACH PLATE ELEMENT IN EXAMPLE 4, METAL BLADE-STIFFENED PANEL WITH THIN SKIN

[Applied loading is $N_x = N_{xy} = 1000.00$ lb/in. (175.13 kN/m)]

Load type	Internal load distribution			
	Plate elements 1 and 3		Plate element 2	
	lb/in.	kN/m	lb/in.	kN/m
N_x	761.23	133.31	883.03	154.64
N_{xy}	1000.00	175.13	0	0

TABLE XI.- VALUES OF FACTOR TO OBTAIN BUCKLING LOADS FOR EXAMPLE 4, METAL BLADE-STIFFENED PANEL WITH THIN SKIN

Applied load				Factor					EAL mode shape
N_x		N_{xy}		VIPASA		Smeared stiffener solution	EAL	STAGS	
lb/in.	kN/m	lb/in.	kN/m	λ = L	λ = L/5, L/6				
0	0	1000	175.1	0.1761	0.2961	0.6062	0.2767	0.2773	Anti
0	0	1000	175.1				.305[a]		Sym
400	70.0	1000	175.1	.1671	.2428	.5541	.2491		Anti
1000	175.1	1000	175.1	.1548	.1840	.4760	.1881		Anti
2000	350.3	1000	175.1	.1374	.1227	.3695	.1253		Anti
4000	700.5	1000	175.1	.1112	.06984	.2222	.07064		Anti
1000	175.1	0	0	.8611	.2958	.9097	.2965		Anti

[a]Second eigenvalue.

Example 5 - Composite Hat-Stiffened Panel

Panel description.- A repeating element of the composite hat-stiffened panel is shown in figure 32. Plate element widths are also shown. The wall construction for each plate element is given in table XII. Only half the laminate is defined for each plate element because all laminates are symmetric. Plate element numbers are indicated by the circled numbers in figure 32. Values for material properties are the same as those used in example 1 and are given in table II. The prebuckling load distribution is given in table XIII. The orthotropic stiffnesses are D_{11} = 242 270 lb-in., D_{22} = 447.77 lb-in., and D_{33} = 8511.2 lb-in.

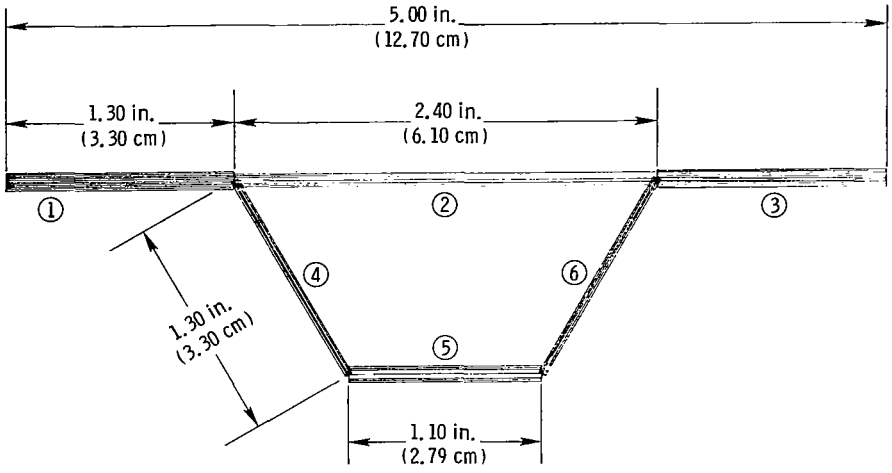

Figure 32.- Repeating element for example 5, composite hat-stiffened panel.

PASCO input and EAL model.- Sample PASCO input for this example is shown in figure 33. (Note that the PASCO input parameter SHEAR is set to 0.3, which indicates that for the smeared stiffener solution, the twisting stiffness D_{33} has been multiplied by 0.3. The reduction is used because the formula for D_{33} is based on the enclosed area of the closed cross section, which, by experience, tends to overestimate the effective stiffness. The value for D_{33} given above is the value after multiplying by 0.3. See refs. 11 and 12.) The finite element type used in the EAL model is the same as that used in the previous models. The finite element grid chosen for the EAL model is shown in figure 34. There are 36 elements along the length. One finite element is used for plate elements 1, 3, and 5, and two finite elements are used for plate elements 2, 4, and 6. There are 1944 finite elements and 1813 nodes.

```
*****  EXAMPLE 5, COMPOSITE HAT-STIFFENED PANEL  *****
 $CONDAT
 $
 $PANEL
 GRANGE=10,
 EL=30,
 B=1.3, 2.4, 1.3, 1.3, 1.1, 1.3,
 T=.010315, .009953, .016955, .025383,
 THET=45, 0, 0, 0,
 KWALL(1,1)= 1,-1,-1,1,2,
 KWALL(1,2)= 1,-1,3,
 KWALL(1,3)= 1,-1,
 KWALL(1,4)= 1,-1,4,
 IWALL=1,2,1,3,4,3,
 HCARD=4,-16,6,60,0,
       4,-14,4,-60,0,
       4,7,14,5,16,
       5,8,1,2,-7,3,
 ICARD=5,1,2,1,-909,0900,
       3,2,5,2,
       3,2,3,14,
       3,3,4,5,
       3,4,5,16,
       3,5,6,3,
       3,6,-909,0900,
 ICREP=6, NOBAY=6,
 MINLAM=30,
 NLAM=1,2,
 SHEAR=.3,
 IBC=1,
 NX=1000.,
 NXY=-1000.,
 $
 $MATER
 E1=19.E6,   E2=1.89E6,  E12=.93E6,  ANU1=.38,  RHO=.0571,
 $
```

Figure 33.- Sample PASCO input for example 5, composite hat-stiffened panel.

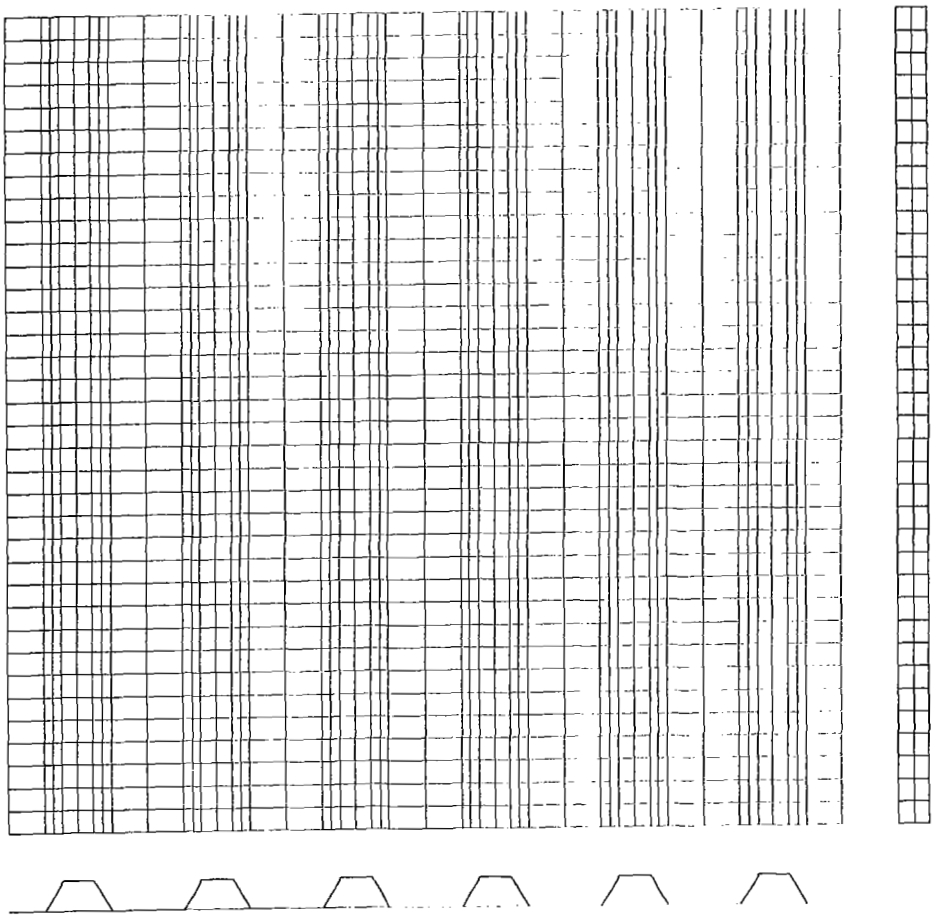

(a) Three views of model.

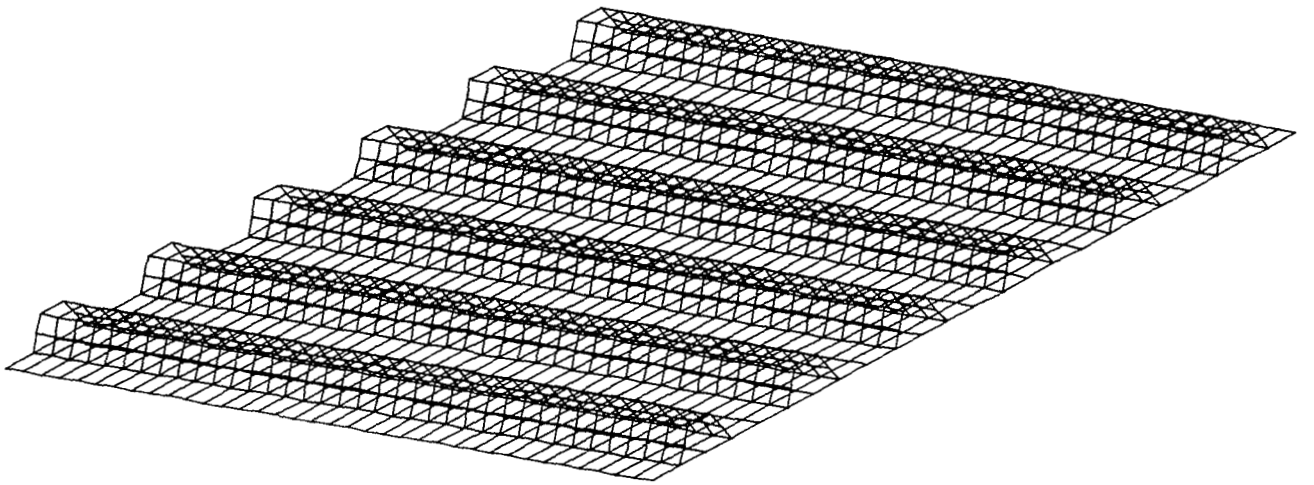

(b) Oblique view.

Figure 34.- EAL finite element model for example 5, composite hat-stiffened panel.

Results.- Buckling results obtained with PASCO and EAL are shown in figure 35. The same general approach used for presenting buckling data in previous examples is used in this example.

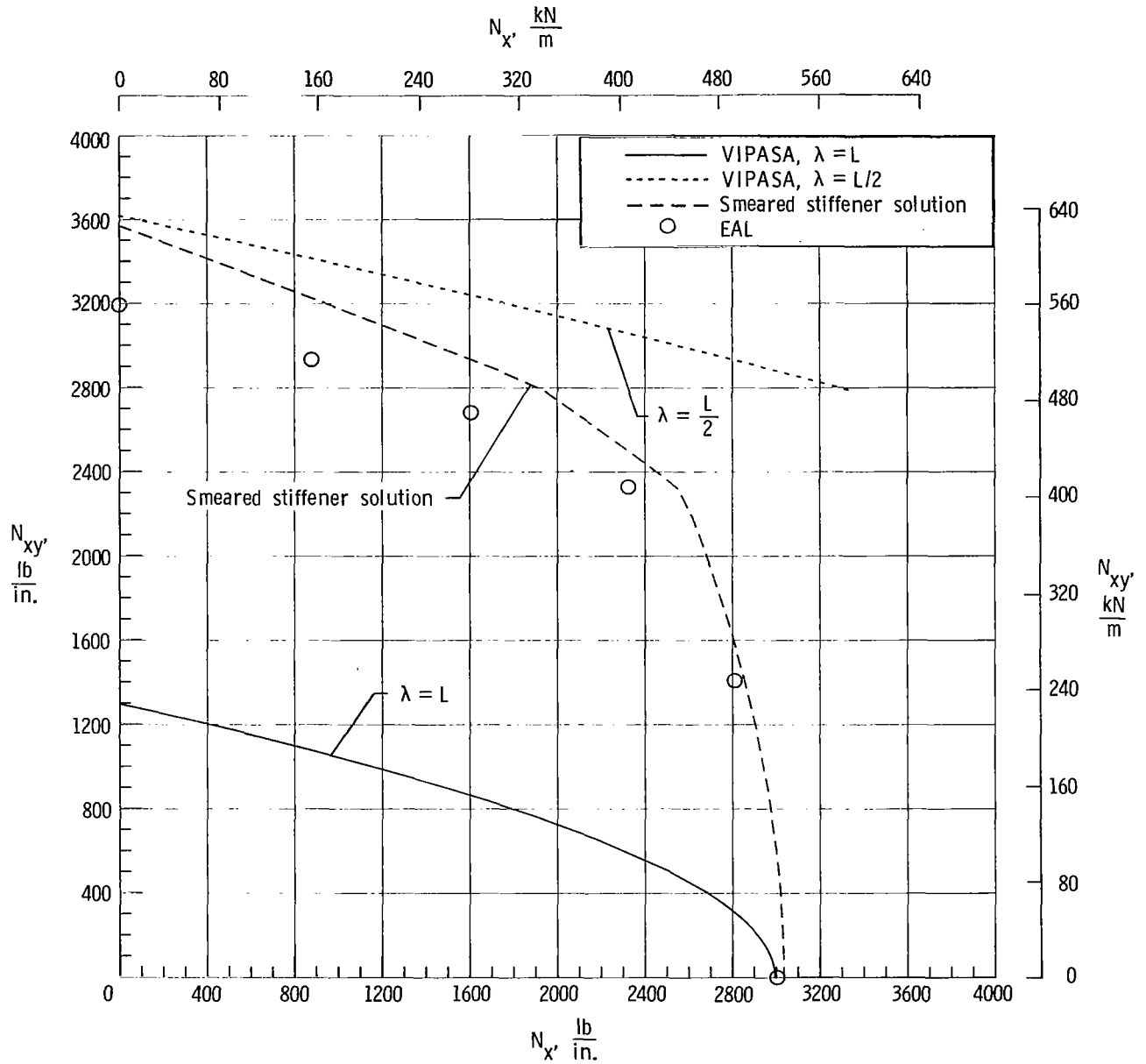

Figure 35.- Buckling load interaction for example 5, composite hat-stiffened panel.

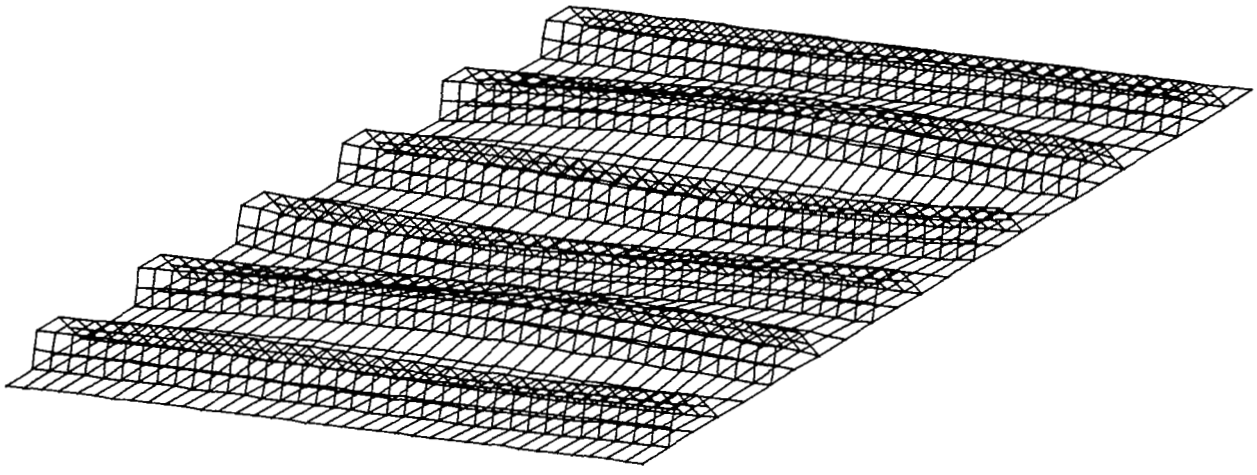

(a) Oblique view.

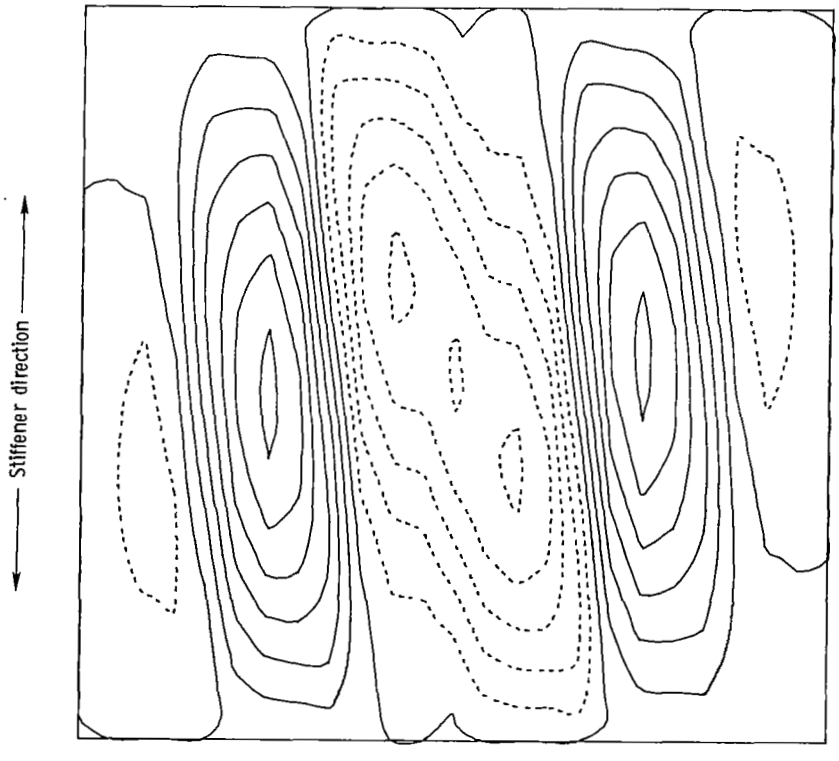

(b) Contour plot.

Figure 36.- Buckling mode shape for pure shear for example 5, composite hat-stiffened panel. Obtained with EAL.

The curve representing the smeared stiffener solution is above the EAL results for the entire range of loadings. If D_{33} had not been reduced by the factor 0.3, the discrepancy would have been even greater. The EAL result for pure shear is an overall mode.

Detailed comparisons of solutions from PASCO and EAL for six loadings are presented in table XIV. The buckling mode shape obtained with EAL for the pure shear loading is shown in figure 36. The buckling mode shapes obtained with EAL and PASCO for the pure compression loading are shown in figure 37.

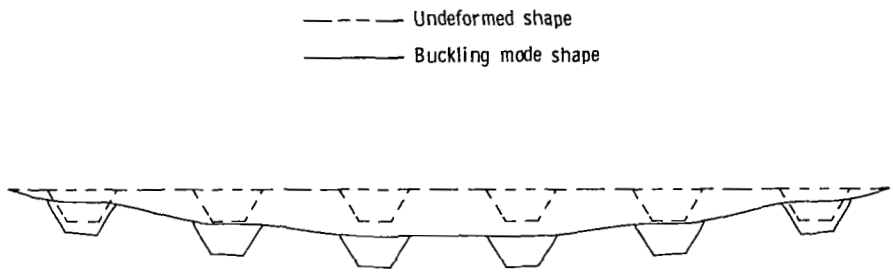

(a) Mode shape obtained with PASCO.

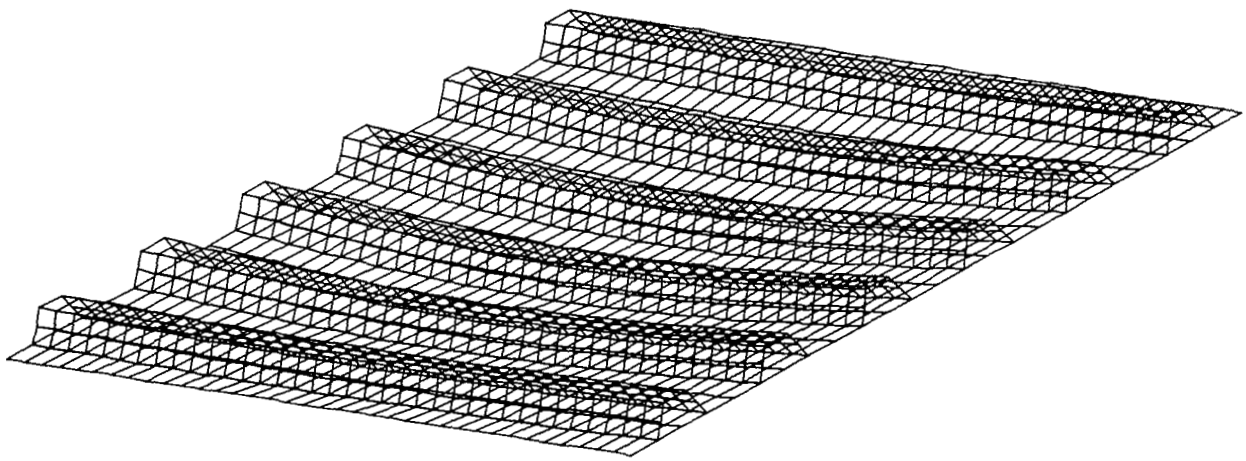

(b) Oblique view of mode shape obtained with EAL.

Figure 37.- Buckling mode shape for pure longitudinal compression for example 5, composite hat-stiffened panel.

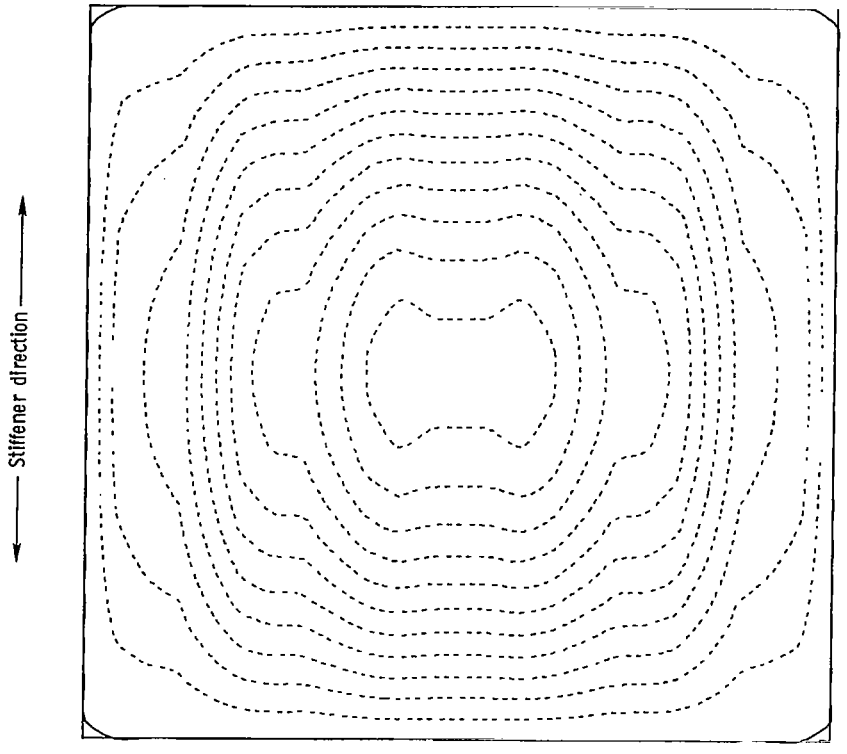

(c) Contour plot of mode shape obtained with EAL.

Figure 37.- Concluded.

TABLE XII.- WALL CONSTRUCTION FOR EACH PLATE ELEMENT IN EXAMPLE 5, COMPOSITE HAT-STIFFENED PANEL

[Only half the laminate is defined for each plate element because all laminates are symmetric]

Layer number, starting with outside layer	Thickness		Fiber orientation, θ, deg
	in.	cm	
Plate elements 1 and 3			
1	0.010315	0.026200	45
2	.010315	.026200	-45
3	.010315	.026200	-45
4	.010315	.026200	45
5	.009953	.025281	0
Plate element 2			
1	0.010315	0.026200	45
2	.010315	.026200	-45
3	.016955	.043066	0
Plate elements 4 and 6			
1	0.010315	0.026200	45
2	.010315	.026200	-45
Plate element 5			
1	0.010315	0.026200	45
2	.010315	.026200	-45
3	.025383	.064473	0

TABLE XIII.- PREBUCKLING LOAD DISTRIBUTION FOR EACH PLATE ELEMENT IN EXAMPLE 5, COMPOSITE HAT-STIFFENED PANEL

[Applied loading is $N_x = N_{xy}$ = 1000.00 lb/in. (175.13 kN/m)]

Load type	Internal load distribution							
	Plate elements 1 and 3		Plate element 2		Plate elements 4 and 6		Plate element 5	
	lb/in.	kN/m	lb/in.	kN/m	lb/in.	kN/m	lb/in.	kN/m
N_x	631.51	110.59	764.63	133.91	128.89	22.57	1079.87	189.11
N_{xy}	1000.00	175.13	626.98	109.80	373.02	65.33	373.02	65.33

TABLE XIV.- VALUES OF FACTOR TO OBTAIN BUCKLING LOADS FOR EXAMPLE 5, COMPOSITE HAT-STIFFENED PANEL

Applied load				Factor				EAL mode shape
N_x		N_{xy}		VIPASA		Smeared stiffener solution	EAL	
lb/in.	kN/m	lb/in.	kN/m	λ = L	λ = L/2			
0	0	1000	175.1	1.2906	3.5433	3.5698	3.192	Sym
300	52.5	1000	175.1	1.2045	3.3203	3.1933	2.932	Sym
600	105.1	1000	175.1	1.1258	3.1147	2.8822	2.680	Anti
1000	175.1	1000	175.1	1.0313	2.8656	2.4229	2.3268	Sym
2000	350.3	1000	175.1	.8385	2.3525	1.4265	1.4062	Sym
1000	175.1	0	0	2.9952		3.0351	3.0042	Sym

Example 6 - Composite Corrugated Panel

Panel description.- A repeating element of the composite corrugated panel is shown in figure 38. Element widths are also shown. The wall construction for each plate element is given in table XV. Plate element numbers are indicated by the circled numbers in figure 38. Only half the laminate is defined for each plate element because all laminates are symmetric. Values for material properties are the same as those used in example 1 and are given in table II. The prebuckling load distribution is given in table XVI. The orthotropic stiffnesses are D_{11} = 130 930 lb-in., D_{22} = 216.53 lb-in., and D_{33} = 184.74 lb-in.

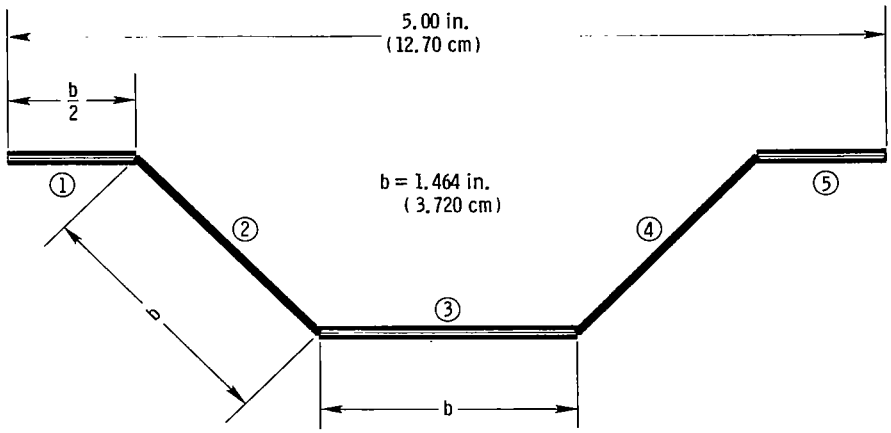

Figure 38.- Repeating element for example 6, composite corrugated panel.

```
*****  EXAMPLE 6, COMPOSITE CORRUGATED PANEL  *****
 $CONDAT
 $
 $PANEL
 EL=30,
 B= .73223,   1.46446,   1.46446,   1.46446,  .73223,
 T=.005479,  .016836,
 THET=45, 0,
 KWALL(1,1)= 1,-1,-1,1,2,
 KWALL(1,2)= 1,-1,-1,1,
 IWALL=1,2,1,2,1,
 HCARD=4,-6,2,-450, -1,
       4,-7,4,450, -1,
       6,8,1,6,3,7,5,
 ICARD=5,1,2,1,-909,0900,
       3,2,3,6,
       3,3,4,3,
       3,4,5,7,
       3,5,6,5,
       3,6,-909,0900,
 ICREP=6,   NOBAY=6,
 MINLAM=30,
 NLAM=1,2,
 SHEAR=1.,
 IBC=1,
 IP=2,
 NX=1000., NXY=-1000.,
 $
 $MATER
 E1=19.E6,   E2=1.89E6,  E12=.93E6,  ANU1=.38,  RHO=.0571,
 $
```

Figure 39.- Sample PASCO input for example 6, composite corrugated panel.

PASCO input and EAL model.- Sample PASCO input for this example is shown in figure 39. The same finite element type used in the EAL model of the first example is used in this example. For the EAL finite element model, shown in figure 40, 36 elements are used down the length of the panel, and 2 elements are used across the width of each plate element.

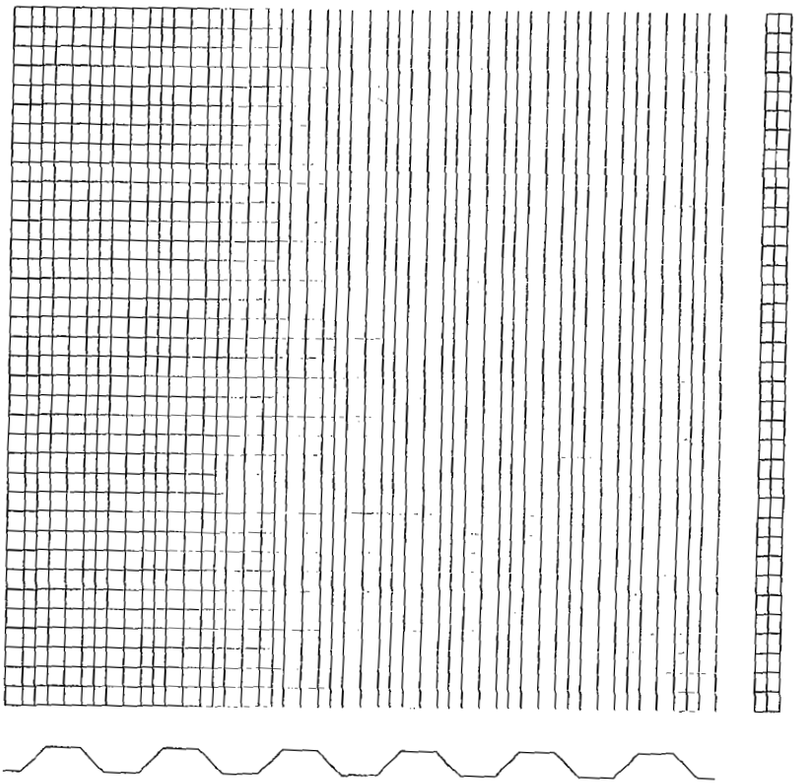

(a) Three views of model.

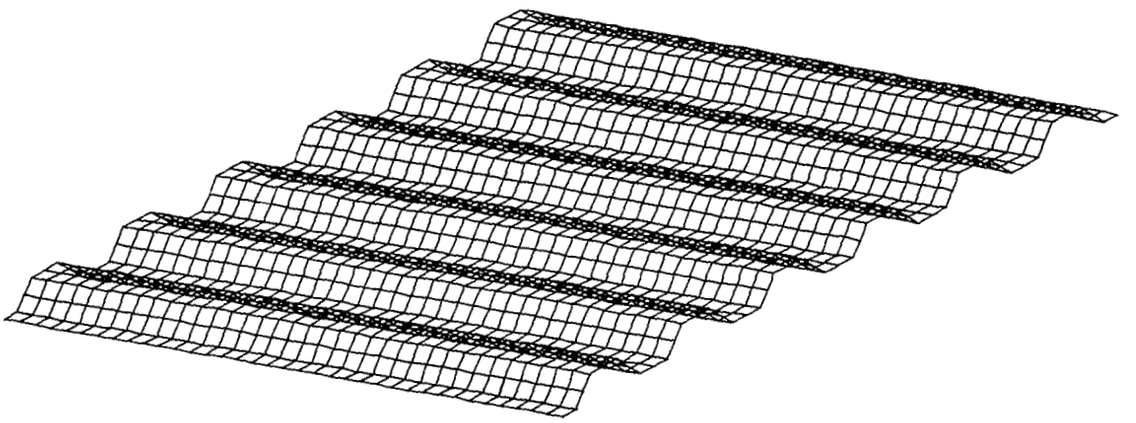

(b) Oblique view of model.

Figure 40.- EAL finite element model for example 6, composite corrugated panel.

Results.- Buckling results obtained with PASCO and EAL for this example are shown in figure 41. The curve for the smeared stiffener solution falls below the EAL results; therefore, for this case, the smeared stiffener approach is conservative. This conservatism exists

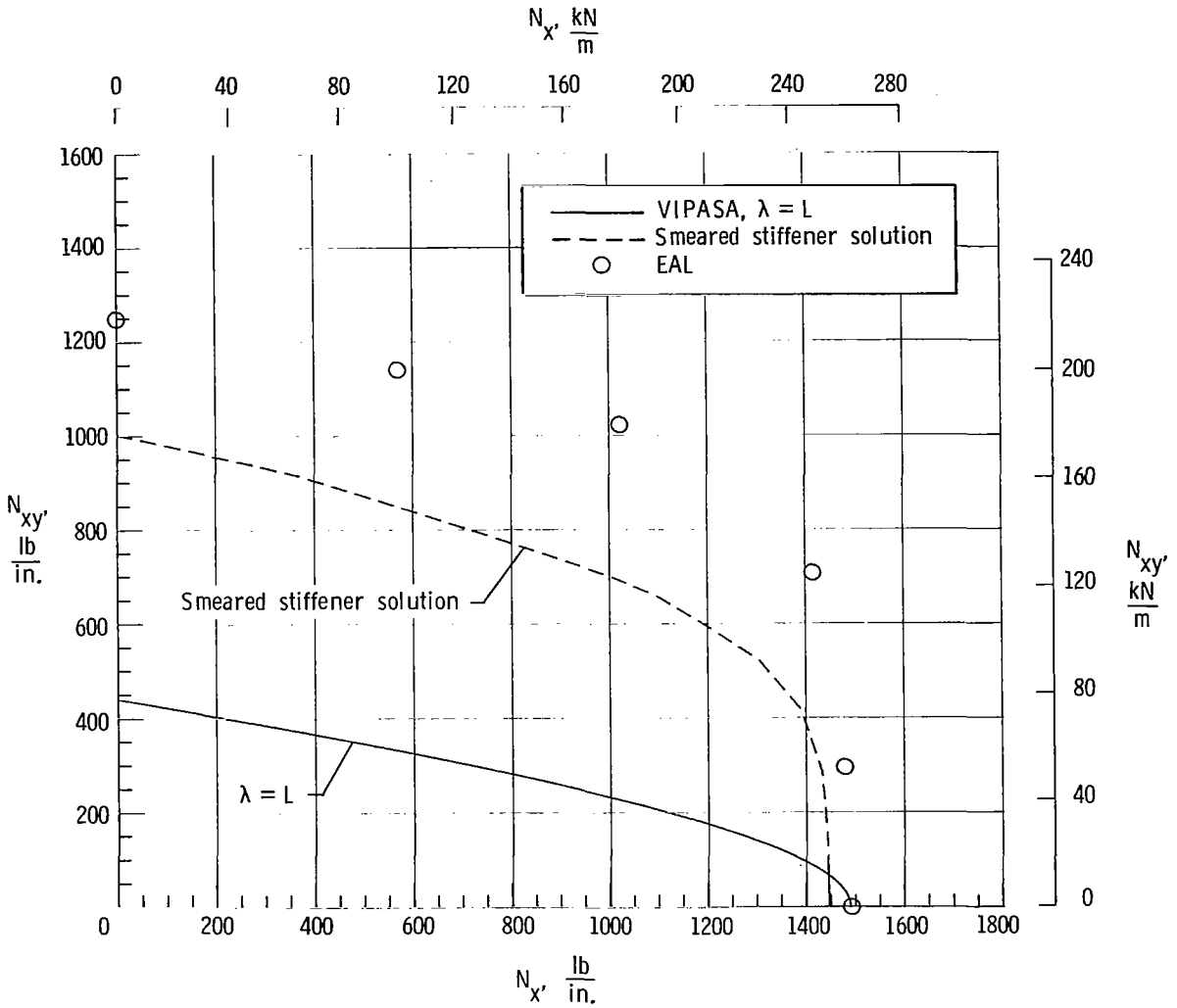

Figure 41.- Buckling load interaction for example 6, composite corrugated panel.

even though the smeared stiffener solution predicts that the buckling half-wavelength transverse to the stiffeners is relatively small. For example, for the pure shear case, the smeared stiffener solution predicts that the buckling half-wavelength transverse to the stiffeners is only 1.2 times the stiffener spacing, which, for this case, is the corrugation pitch. Results from the other examples suggest that a buckling half-wavelength of only 1.2 times the stiffener spacing would cause the smeared stiffener solution to be very unconservative; that is, the solution would overestimate the buckling load. The buckling mode shape for the pure shear case, figure 42, shows that buckling is limited to the area near the side edges.

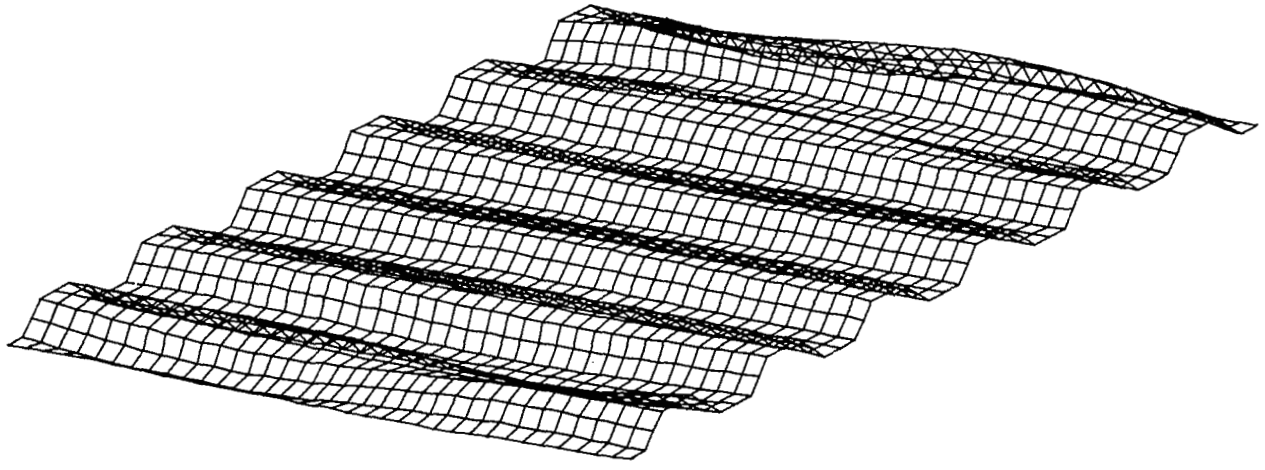

Figure 42.- Buckling mode shape for pure shear for example 6, composite corrugated panel. Obtained with EAL.

Because these results do not fit the pattern of results from the other examples, several additional calculations were made. First, the correct simple support boundary conditions were applied to the sides of the smeared stiffener model. However, imposing these boundary conditions increased the buckling load by only about 3 percent for the pure shear case.

Next, it was thought that the location of the side supports on the EAL model was causing the EAL buckling load to be larger than it would be for supports at other locations. To explore that possibility, a second EAL model was constructed. That model is identical to the original model except that the supports are shifted one quarter period to the right, as shown in figure 43. In the new model, the supports are at the midheight of the cross section. Calculations with the new model showed that, instead of being smaller, the buckling load for the pure

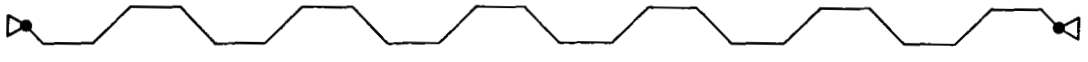

Figure 43.- Corrugated panel modeled with supports at midheight of cross section.

shear loading increased by about 15 percent. As can be seen in figure 44, the buckling mode shape for the second model extends over the entire panel rather than being limited to the area near the side edges, which was the case for the original model (fig. 42).

Another possible reason the smeared stiffener solution underestimates the buckling load for the corrugated panel is that the orthotropic stiffnesses are underestimated. In particular, neglecting restraint of warping may be a factor in underestimating the twisting stiffness. However, the twisting stiffness formula used in the PASCO smeared stiffener solution (eq. (13), ref. 11) includes extra terms which make it larger than the twisting stiffness calculated by many standard approaches, such as the formula on page 367 of reference 18.

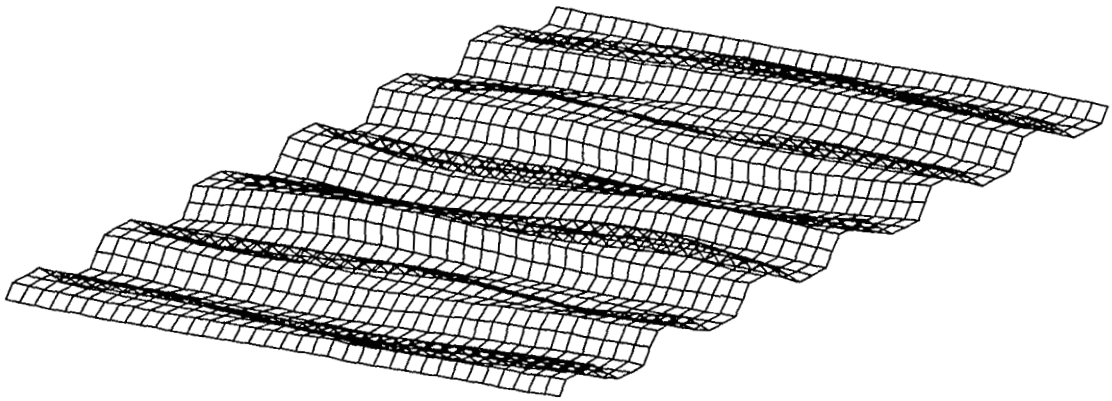

Figure 44.- Buckling mode shape for pure shear for corrugated panel supported as shown in figure 43. Obtained with EAL.

It can only be concluded that although a smeared stiffener solution provides an estimate of the buckling load for an overall mode, it sometimes overestimates the buckling load and sometimes underestimates the load. This simplified approach cannot be counted on to be consistent.

Detailed comparisons of results from PASCO and EAL for six loadings are presented in table XVII. The buckling mode shapes obtained with EAL and PASCO for the pure compression case are shown in figure 45.

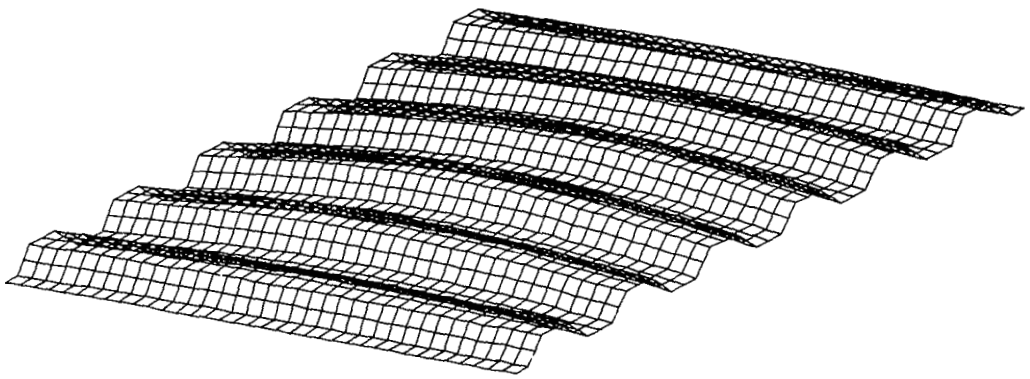

(a) Mode shape obtained with EAL.

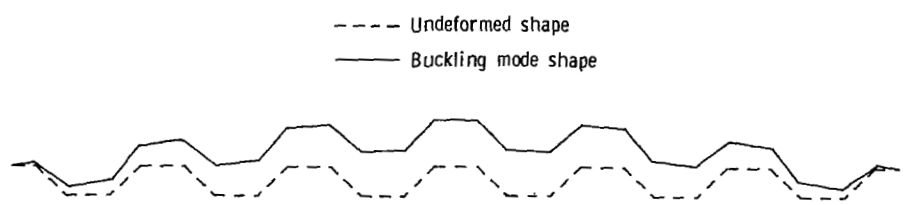

(b) Mode shape obtained with PASCO.

Figure 45.- Buckling mode shape for pure longitudinal compression for example 6, composite corrugated panel.

TABLE XV.- WALL CONSTRUCTION FOR EACH PLATE ELEMENT IN EXAMPLE 6, COMPOSITE CORRUGATED PANEL

[Only half the laminate is defined for each plate element because all laminates are symmetric]

Layer number, starting with outside layer	Thickness		Fiber orientation, θ, deg
	in.	cm	
Plate elements 1, 3, and 5			
1	0.005479	0.013917	45
2	.005479	.013917	-45
3	.005479	.013917	-45
4	.005479	.013917	45
5	.016836	.042763	0
Plate elements 2 and 4			
1	0.005479	0.013917	45
2	.005479	.013917	-45
3	.005479	.013917	-45
4	.005479	.013917	45

TABLE XVI.- PREBUCKLING LOAD DISTRIBUTION FOR EACH PLATE ELEMENT IN EXAMPLE 6, COMPOSITE CORRUGATED PANEL

[Applied loading is $N_x = N_{xy} = 1000.00$ lb/in. (175.13 kN/m)]

Load type	Internal load distribution			
	Plate elements 1, 3, and 5		Plate elements 2 and 4	
	lb/in.	kN/m	lb/in.	kN/m
N_x	1448.89	253.74	258.22	45.22
N_{xy}	1000.00	175.13	1000.00	175.13

TABLE XVII.- VALUES OF FACTOR TO OBTAIN BUCKLING LOADS FOR EXAMPLE 6, COMPOSITE CORRUGATED PANEL

Applied load				Factor		
N_x		N_{xy}		VIPASA	Smeared stiffener solution	EAL
lb/in.	kN/m	lb/in.	kN/m	$\lambda = L$		
0	0	1000	175.1	0.4371	1.0011	1.248
500	87.6	1000	175.1	.4010	.8894	1.1395
1000	175.1	1000	175.1	.3692	.7780	1.0223
2000	350.3	1000	175.1	.3161	.5971	.7077
5000	875.6	1000	175.1	.2131	.2865	.2958
1000	175.1	0	0	1.4897	1.4462	1.4918

Example 7 - Metal Z-Stiffened Panel

Panel description.- A repeating element of the metal Z-stiffened panel is shown in figure 46. Element widths and thicknesses are also shown. The material properties used in the

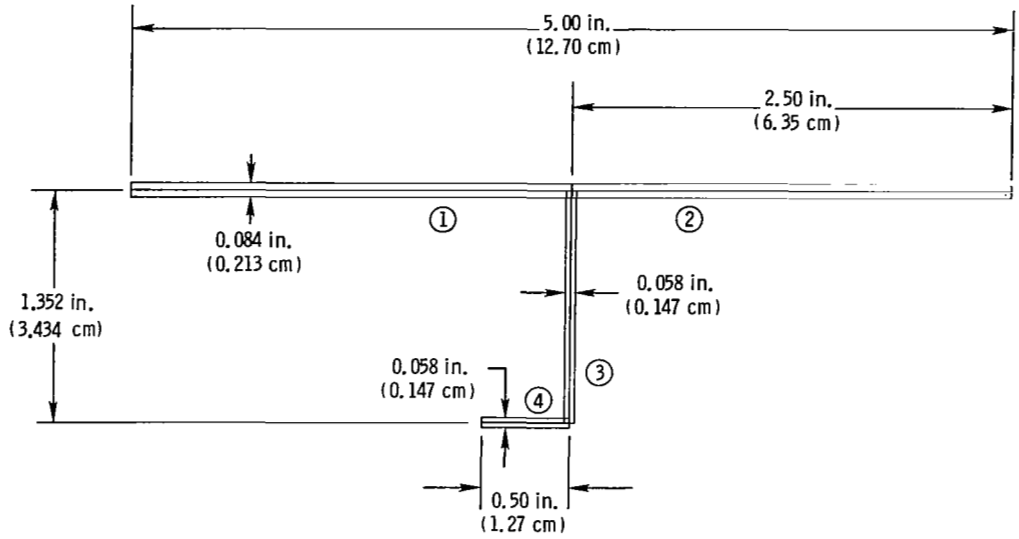

Figure 46.- Repeating element for example 7, metal Z-stiffened panel.

```
*****  EXAMPLE 7, METAL Z-STIFFENED PANEL  *****
 $CONDAT
 $
 $PANEL
 B=2.5, 1.352, 2.5, .5,
 T=.042, .029,
 THET= 0, 0,
 KWALL(1,1)=1,
 KWALL(1,2)=2,
 IWALL=1,2,1,2,
 HCARD=4,-5,2,90,0,
       3,121,4,5,
       4,6,1,3,-121,
 ICARD=5,1,4,1,-909,0900,
       3,3,4,5,
       3,2,3,4,
       3,4,5,3,
       3,5,-909,0900,
 ICREP=6,
 NOBAY=6,
 EL=30,
 MINLAM=30,
 NLAM=1,2,5,6,
 SHEAR=1.,
 IBC=1,
 IP=2,
 NX=1000.,
 NXY=-1000.,
 $
 $MATER
 E1=10.5E6, E2=10.5E6, E12=3.9772727E6, ANU1=.32, RHO=.1,
 $
 $
```

Figure 47.- Sample PASCO input for example 7, metal Z-stiffened panel.

calculations are $E = 10.5 \times 10^6$ psi (72.4 GPa), $\mu = 0.32$. Except for the addition of the flange on the stiffener, this panel is the same as that used in example 2. The prebuckling load distribution is given in table XVIII. The orthotropic stiffnesses are $D_{11} = 178\ 390$ lb-in., $D_{22} = 578.07$ lb-in., and $D_{33} = 324.11$ lb-in.

PASCO input and EAL model.- PASCO input for this example is presented in figure 47. The same basic finite element grid pattern used in the EAL model of the first example is used in this example. The flange (plate element 4) is modeled with a single element across the width.

Results.- Buckling results obtained with PASCO and EAL are shown in figure 48. The same general approach used for presenting buckling data in previous examples is used in this example. Curves indicate PASCO results, and symbols indicate EAL results. The results for this example are similar, in many ways, to the results for example 4.

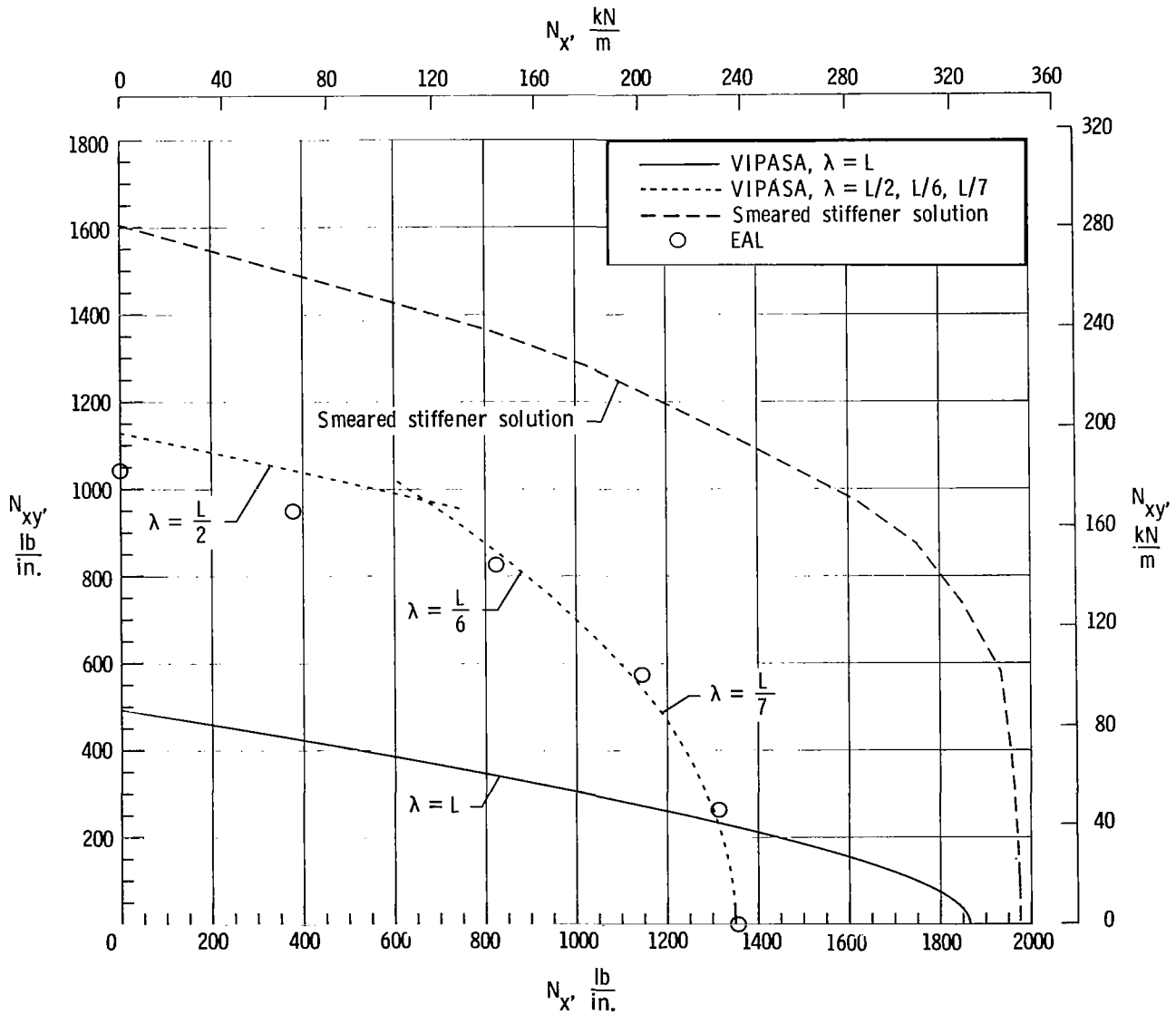

Figure 48.- Buckling load interaction for example 7, metal Z-stiffened panel.

The solid curve represents the standard VIPASA solution for $\lambda = L$. The dotted curve represents the standard VIPASA solutions for $\lambda = L/2$, $L/6$, and $L/7$. The dashed curve represents the smeared stiffener solution. For the pure shear loading, the smeared stiffener solution has a buckling half-wavelength transverse to the stiffeners that is 1.5 times the stiffener spacing.

Detailed comparisons of solutions from PASCO and EAL for six loadings are presented in table XIX. The buckling mode shape obtained with EAL for the pure shear loading is shown in figure 49. Note that because of the flange, the stiffener is unsymmetric; therefore,

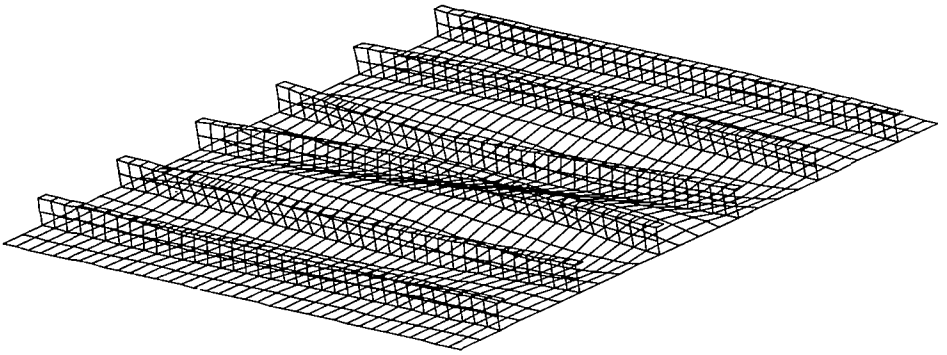

(a) Oblique view.

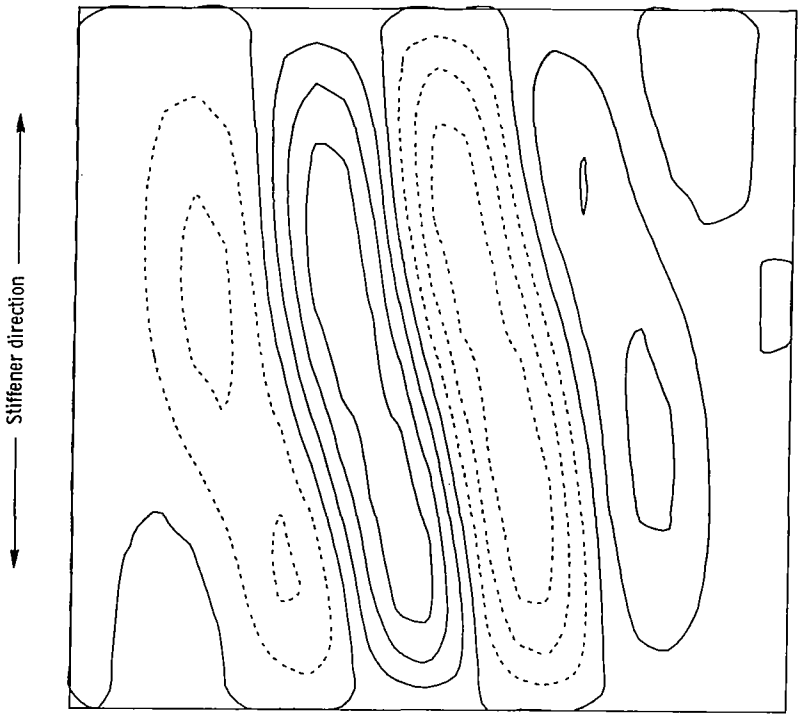

(b) Contour plot.

Figure 49.- Buckling mode shape for pure shear for example 7, metal Z-stiffened panel. Obtained with EAL.

buckling mode shapes are neither perfectly symmetric nor perfectly antisymmetric. The buckling mode shapes obtained with PASCO and EAL for pure compression are shown in figure 50.

(a) Mode shape obtained with PASCO.

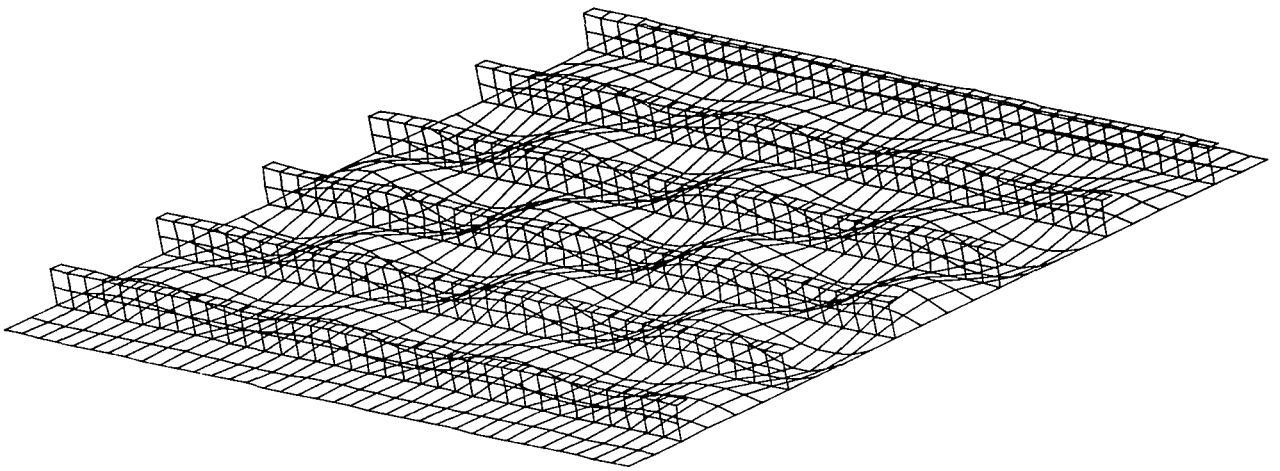

(b) Oblique view of mode shape obtained with EAL.

Figure 50.- Buckling mode shape for pure longitudinal compression for example 7, metal Z-stiffened panel.

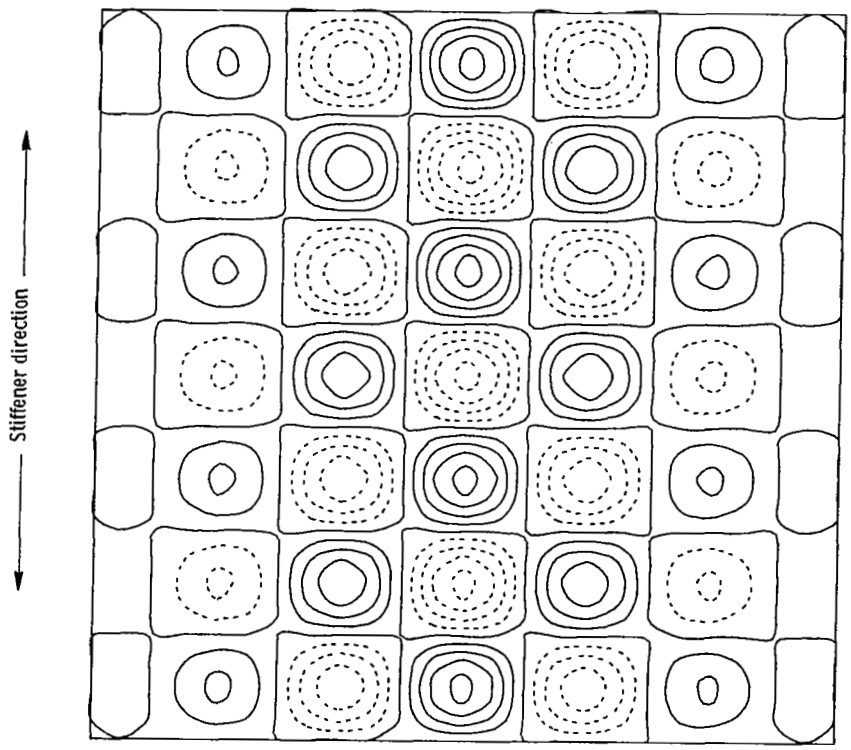

(c) Contour plot of mode shape obtained with EAL.

Figure 50.- Concluded.

TABLE XVIII.- PREBUCKLING LOAD DISTRIBUTION FOR EACH PLATE ELEMENT IN EXAMPLE 7, METAL Z-STIFFENED PANEL

[Applied loading is $N_x = N_{xy} = 1000.00$ lb/in. (175.13 kN/m)]

Load type	Internal load distribution			
	Plate elements 1 and 2		Plate elements 3 and 4	
	lb/in.	kN/m	lb/in.	kN/m
N_x	796.34	139.46	549.85	96.29
N_{xy}	1000.00	175.13	0	0

TABLE XIX.- VALUES OF FACTOR TO OBTAIN BUCKLING LOADS FOR EXAMPLE 7, METAL Z-STIFFENED PANEL

Applied load				Factor					EAL mode shape
N_x		N_{xy}		VIPASA			Smeared stiffener solution	EAL	
lb/in.	kN/m	lb/in.	kN/m	$\lambda = L$	$\lambda = L/2$	$\lambda = L/6, L/7$			
0	0	1000	175.1	0.4924	1.1282		1.6050	1.042	Anti
400	70.0	1000	175.1	.4606	1.0336		1.4343	.948	Anti
1000	175.1	1000	175.1	.4186	.9123	0.8420	1.1966	.825	Anti
1000	175.1	500	87.6	.7224		1.1292	1.7501	1.146	Anti
1000	175.1	200	35.0	1.2473		1.3039	1.9579	1.315	Sym
1000	175.1	0	0	1.8662		1.3503	1.9768	1.356	Sym

RECENT DEVELOPMENTS

During the final stages of preparation of this paper, a closely related paper dealing with the buckling analysis of shear-loaded stiffened panels was published. In that paper (ref. 19), a method is presented for enforcing desired support conditions along the ends of stiffened panels loaded in shear. The method combines Lagrangian multipliers, which are used to impose the support conditions, and the computer program VIPASA (refs. 1 to 3). The method described in reference 19 has been incorporated in a computer program denoted VICON.

VICON retains many of the advantages and computational efficiencies of the VIPASA program. VICON can calculate the buckling load of a stiffened panel with rather general rigid and elastic supports. In particular, VICON can be used when the buckling mode shape is required to have zero deflection along a rectangular boundary. In one calculation presented in reference 19, VICON is shown to give results in good agreement with EAL for example 2 of this paper.

CONCLUDING REMARKS

Buckling results obtained with several buckling analysis procedures are presented in this paper for seven stiffened panels. Four of the panels are blade-stiffened panels. One panel has a small flange at the tip of each blade to produce a Z-stiffened panel. One panel has hat stiffeners, and one panel is a corrugated panel. Four of the panels are made of graphite-epoxy; three panels are made of aluminum. The analysis procedures used to calculate buckling loads are the computer program PASCO, which includes both a linked-plate analysis procedure denoted VIPASA and a smeared stiffener solution, and two finite element computer programs, EAL and STAGS. For one panel, additional solutions for local buckling are obtained from simple formulas.

The paper has two primary objectives: to examine the validity of the smeared stiffener solution and to provide a set of accurate benchmark calculations for evaluating other analysis procedures. A third objective is to provide insight into the buckling characteristics of stiffened panels. Numerous figures showing buckling mode shapes are included to help accomplish this third objective.

A smeared stiffener solution is obtained by averaging or "smearing" the stiffnesses of the stiffeners over the panel. The result is an equivalent orthotropic plate that can be analyzed with relatively simple procedures. A smeared stiffener solution is only used when it is assumed that the buckling mode shape has a buckling wave that extends over several stiffeners. The buckling results presented in this paper indicate that the smeared stiffener solution should be used only with caution. Inaccuracies arise for at least two reasons. First, it may be difficult to calculate the proper orthotropic stiffnesses - particularly the twisting stiffness. Second, local stiffener deformations are ignored. These local deformations can

be important even when the buckling wave extends over several stiffeners. In the results presented in this paper, the smeared stiffener solution generally predicted a buckling load that was higher than the buckling load predicted by the more accurate analyses.

Another conclusion of this study is that a PASCO solution can be very helpful when developing an adequate finite element model. Because PASCO is essentially exact for certain loadings and boundary conditions, the adequacy of a finite element solution (e.g., modeling detail, element capability, and eigenvalue solution) can be checked by comparing the finite element solution with the PASCO solution for a loading system and set of boundary conditions known to be exact in PASCO. Once the finite element procedure is determined to be adequate for the check case, the finite element analysis can be carried out with the desired loading and boundary conditions. Although this approach does not guarantee an accurate solution for the new loadings and boundary conditions, it can quickly point out deficiencies.

Finally, these results are for buckling of perfect panels. All real panels have imperfections that reduce their buckling loads. Analysis procedures can generally account for some of these imperfections. Also, buckling does not necessarily mean failure. For some panels and loadings, material strength failures occur before the buckling load is reached. Other panels may have substantial postbuckling strength. Still, an accurate prediction of the buckling load can be important in understanding the behavior of stiffened panels.

Langley Research Center
National Aeronautics and Space Administration
Hampton, VA 23665
October 24, 1983

APPENDIX

EAL RUNSTREAMS USED FOR PANEL ANALYSES

The EAL runstreams used to carry out the panel studies are included in this section. An EAL runstream is somewhat analogous to a FORTRAN subroutine in that it consists of a collection of stored EAL input statements that can be processed by invoking a single command. Several of the runstreams are quite general and can be used in the analysis of any prismatic, plate-type structure composed of repeating elements. These runstreams were used for all panel configurations considered in this paper. To illustrate the use of these more general runstreams in performing a panel buckling analysis, the specific input is presented for example 1, the composite blade-stiffened panel.

The input for the panel buckling analyses consists of a set of commands which initiate the execution of various EAL runstreams which, in turn, call other lower level runstreams. The execution flow and the runstreams for example 1 are described by starting with the highest level and proceeding to the lower level, general purpose runstreams.

The following commands control the execution of the example 1 buckling analysis:

*CALL (PANEL, BLADE)

*CALL (PANEL, GEOM)

*CALL (SA, BLADE)

*CALL (PANEL, BUCK)

where the *CALL command merely begins execution of the runstream named between parentheses.

Runstream PANEL, BLADE

The runstream PANEL, BLADE, which is shown in figure A1, applies specifically to the particular problem being solved - in this case, the composite blade-stiffened panel (example 1) under a pure compression load. The main purpose of the runstream is to define several EAL tables used by the general purpose runstreams, which generate the panel geometry and directly apply the prebuckling stress state. The register NMNX defines the number of nodes to be generated along the panel length. The register NREP defines the number of repeating elements to be replicated in the direction of panel width. The data set STRES TABLE contains a line of N_x, N_y, and N_{xy} values for each different plate wall in the panel cross section. In this case, the skin is assigned section property 1, and the blade is assigned property 2.

The purpose of data set JLOC REPE is to set up a list of local y, z coordinate values for a set of joints in the repeating element cross section. The seven joints used to define the finite element representation of the repeating element are shown in figure A2. In generating this table for example 1, heavy use is made of the EAL "register" capability to allow for

simple changes to the dimensions of the panel cross section. The data set EDEF REPE defines the element connectivities and section properties for the repeating element. The joint numbers used to define the element connectivities are the same local numbers defined in JLOC REPE. The six elements defined in EDEF REPE are designated by the circled numbers in figure A2. In EDEF REPE there are four integer entries for each defined element. The first two entries are local node numbers for the repeating element. These two numbers define a line and, together with NMNX, are used to generate a row (in the x-direction) of E43 elements. The third integer points to the material property data in data set MATC BTAB for this element, and the fourth integer points to the wall section property data in data set SA BTAB.

Runstream PANEL, GEOM

The runstream PANEL, GEOM (fig. A3) is the driver runstream for constructing the panel geometry information. It calls the general runstream PANEL, JLOC (fig. A4), which uses primarily the data set JLOC REPE to produce joint location data for all repeating elements in the panel. PANEL, GEOM also calls runstream PANEL, ELD (fig. A5), which uses primarily the data set EDEF REPE to define all the two-dimensional E43 elements in the panel. Boundary condition information is defined in PANEL, GEOM with subprocessor CON in processor TAB. The commands under CON 1 define classical simple support boundary conditions for the nodes on all four panel edges including the stiffeners. Material property and wall section property information can also be defined in PANEL, GEOM, as is done here. For this particular example, since it contains composite laminates, the wall section properties are defined in a separate runstream SA, BLADE (fig. A6). Thus, the SA section property data produced by runstream SA, BLADE supersede that produced in PANEL, GEOM.

Runstream PANEL, BUCK

The runstream PANEL, BUCK (fig. A7) actually performs the buckling analysis of the panel defined with the previously described runstreams. It calls runstream PANEL, LOADS (fig. A8), which uses the data sets EDEF REPE and STRES TABLE to directly apply the prebuckling stress state to every E43 element in the panel. Then, linear and geometric stiffness matrices are produced and the eigenvalue problem solved. As shown, PANEL, BUCK is written to solve a shifted eigenvalue problem based on the value of register SHIFT. SHIFT, used to speed convergence, is merely a guess at the lowest eigenvalue and can be set to zero.

APPENDIX

```
*(28,PANEL,BLADE) ABC
*XQT AUS
$
$ RUNSTREAM THAT PREPARES GEOMETRY DESCRIPTION AND PRE-BUCKLING
$ STRESS RESULTANT TABLES FOR EXAMPLE 1.
$
!  NMNX=37
!  NREP=6
!  LPAN=30.
!  B=5.0
!  D=1.352
!SHIFT=.93
TABLE(NI=3,NJ=2) : STRES TABLE
J=1 : -811.35 0.  0.
J=2 : -697.67 0.  0.
TABLE(NI=2,NJ=7) : JLOC REPE
!  BO2=B/2.
!  BO4=B/4.
!  BO34=3.*BO4
!  DO2=D/2.0
J=1,7
0.  0.  $ 1
"BO4" 0.  $ 2
"BO2" 0.  $ 3
"BO2" "DO2" $ 4
"BO2" "D" $ 5
"BO34" 0.  $ 6
"B" 0.  $ 7
TABLE(NI=4,NJ=6,RMODE=2,TYPE=0) : EDEF REPE
J=1,6
1 2 1 1
2 3 1 1
3 4 1 2
4 5 1 2
3 6 1 1
6 7 1 1
*RETURN
* ABC
```

Figure A1.- Listing of runstream PANEL, BLADE.

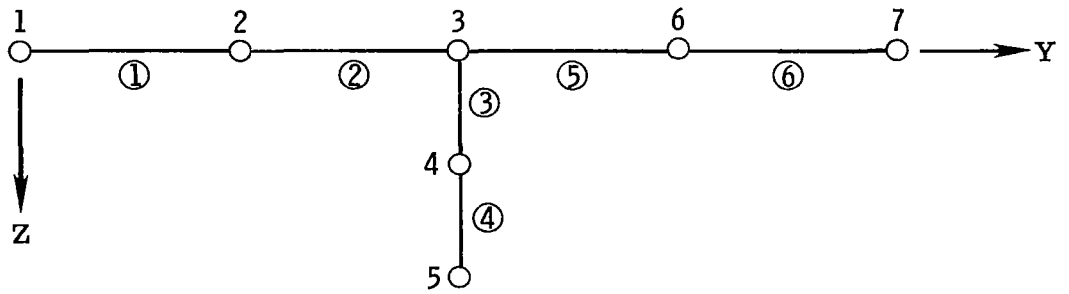

Figure A2.- EAL repeating element for example 1 with local joint and element numbers.

```
*(28,PANEL,GEOM) ABC
*XQT DCU
$
$ GENERAL RUNSTREAM THAT CREATES THE PANEL GEOMETRY
$
PRINT 1 JLOC REPE
PRINT 1 EDEF REPE
PRINT 1 STRESS TABLE
*CALL(PANEL,JLOC)
*XQT TAB
MATC : 1 10.5+6 .32 .101
SA
1 .084
2 .058
3 .058
4 1.0
CON 1
!  MM1 = NUMN - NMNX + 1
ZERO 2,3,4 : 1, "MM1" "NMNX"
ZERO 2,3,4 : "NMNX" "NUMN" "NMNX"
ZERO 1,3,5 : "MM1" "NUMN" $ SIMPLE SUPPORT
ZERO 1,3,5 : 1,"NMNX" $ SIMPLE SUPPORT
*CALL(PANEL,ELD)
*RETURN
* ABC
```

Figure A3.- Listing of runstream PANEL, GEOM.

```
*(28,PANEL,JLOC) ABC
*XQTC U1
$
$ A GENERAL RUNSTREAM TO CREATE JOINT LOCATION DATA FOR A PRISMATIC
$ STRUCTURE COMPOSED OF REPEATING ELEMENTS.
$
$ INPUT DATA SET :
$ JLOC REPE 1 1 - TABLE DEFINING NODES IN REPEATING ELEMENT CROSS SECTION
$
*REGISTER EXCEPTIONS= NMNX, NREP, LPAN
*REGISTER STORE(15 HOLD REG 1 1)
$ NMNX - NUMBER OF NODES IN LENGTH DIRECTION
$ NREP - NUMBER OF REPEATING ELEMENTS
$ LPAN - LENGTH OF THE PRISMATIC STRUCTURE
$
!  NNRE= TOC,NJ(1,JLOC,REPE,1,1) $ NUMBER OF NODES IN REPEATING CROSS SECTION
!  NUMN= NNRE-1 : !NUMN= NUMN*NMNX*NREP + NMNX
!  NNRE : !  NUMN
*XQT TAB
START "NUMN"
JOINT LOCATIONS
!  YBASE=0.0 : !  DELY=DS,1,"NNRE",1(1,JLOC,REPE,1,1)
!  JBASE=0 : !  DELN=NNRE*NMNX-NMNX
$
$ LOOP OVER ALL REPEATING ELEMENTS
$
!  CNT1=NREP
*LABEL RELOOP
$
$ LOOP OVER THE CROSS SECTION NODES IN THE REPEATING ELEMENT
$
!  CNT2=NNRE
!  JJ=1
*LABEL NDLOOP
!  Y=DS,1,"JJ",1(1,JLOC,REPE,1,1) : !  Y= Y+YBASE
!  Z=DS,2,"JJ",1(1,JLOC,REPE,1,1)
!  JNT= JJ*NMNX - NMNX + 1 + JBASE
$
"JNT" 0.  "Y" "Z" "LPAN" "Y" "Z" "NMNX"
$
!  JJ=JJ+1
*JGZ,-1(CNT2,NDLOOP)
$
!  JBASE=JBASE+DELN
!  YBASE=YBASE+DELY
*JGZ,-1(CNT1,RELOOP)
*XQT U1
*REGISTER EXCEPTIONS= NUMN
*REGISTER RETRIEVE(15 HOLD REG 1 1)
*RETURN
* ABC
```

Figure A4.- Listing of runstream PANEL, JLOC.

```
*(28,PANEL,ELD) ABC
*XQTC U1
$
$ A GENERAL RUNSTREAM TO CREATE ELEMENT DEFINITION DATA FOR A PRISMATIC
$ STRUCTURE COMPOSED OF REPEATING ELEMENTS.
$
$ INPUT DATA SET :
$ EDEF REPE 1 1 - TABLE DEFINING ELEMENT CONNECTIVITY IN THE
$ CROSS SECTION OF THE REPEATING ELEMENT
*REGISTER EXCEPTIONS=NREP, NMNX
*REGISTER STORE(15 HOLD REG 1 1)
$ NREP - NUMBER OF REPEATING ELEMENTS
$ NMNX - NUMBER OF NODES IN THE LENGTH DIRECTION
$
*XQT ELD
E43
!  NNRE=TOC,NJ(1,JLOC,REPE,1,1)
!  NERE=TOC,NJ(1,EDEF,REPE,1,1) $ NUMBER OF ELEMENTS IN REPEATING CROSS SECTION
!  NELX=NMNX-1
!  JBASE=0 : !  DELN=NNRE*NMNX-NMNX
$
$ LOOP OVER ALL REPEATING ELEMENTS IN THE STRUCTURE
$
!CNT1=NREP
*LABEL RELOOP
$
$ LOOP OVER ALL ELEMENTS IN THE REPEATING ELEMENT
$
!  CNT2=NERE
!  JJ=1
*LABEL NELOOP
!  J1= DS,1,"JJ",1(1,EDEF,REPE,1,1)
!  J2= DS,2,"JJ",1(1,EDEF,REPE,1,1)
!  N1= J1*NMNX - NMNX + 1 + JBASE
!  N4= J2*NMNX - NMNX + 1 + JBASE
!  N2= N1+1
!  N3= N4+1
!  NMAT = DS,3,"JJ",1(1,EDEF,REPE,1,1)
!  NSECT = DS,4,"JJ",1(1,EDEF,REPE,1,1)
$
NMAT="NMAT" : NSECT="NSECT"
$
"N1" "N2" "N3" "N4" 1 "NELX"
$
!  JJ=JJ+1
*JGZ,-1(CNT2,NELOOP)
!  JBASE=JBASE+DELN
*JGZ,-1(CNT1,RELOOP)
*XQT U1
*REGISTER RETRIEVE(15 HOLD REG 1 1)
*RETURN
* ABC
```

Figure A5.- Listing of runstream PANEL, ELD.

```
*(28,SA,BLADE) ABC
*XQT AUS
$
$ RUNSTREAM THAT CREATES LAMINATE PROPERTIES FOR EXAMPLE 1.
$
TABLE(NI=9,NJ=3) : OMA DATA 0 0
J=1 : 19.+6 1.89+6 .38 .93+6 .0055 0.  0.  0.  0.  $
J=2 : 19.+6 1.89+6 .38 .93+6 .0495 0.  0.  0.  0.  $
J=3 : 19.+6 1.89+6 .38 .93+6 .0110 0.  0.  0.  0.  $
TABLE(NI=2,NJ=12) : LAM OMA 1 0 $ PANEL SKIN
J=1 : 1.  45.
J=2 : 1.  -45.
J=3 : 1.  -45.
J=4 : 1.  45.
J=5 : 1.  0.
J=6 : 2.  90.
J=7 : 2.  90.
J=8 : 1.  0.
J=9 : 1.  45.
J=10 : 1.  -45.
J=11 : 1.  -45.
J=12 : 1.  45.
TABLE(NI=2,NJ=10) : LAM OMA 2 0 $ BLADE STIFFENERS
J=1 : 1.  45.
J=2 : 1.  -45.
J=3 : 1.  -45.
J=4 : 1.  45.
J=5 : 3.  0.
J=6 : 3.  0.
J=7 : 1.  45.
J=8 : 1.  -45.
J=9 : 1.  -45.
J=10 : 1.  45.
*XQT TAB
SA(OMAL=1,MAXNL=12)
*RETURN
* ABC
```

Figure A6.- Listing of runstream SA, BLADE.

```
*(28,PANEL,BUCK) ABC
$
$ GENERAL RUNSTREAM TO FORM STIFFNESS MATRICES AND SOLVE THE
$ BUCKLING EIGENVALUE PROBLEM.
$
*XQT E
*XQT EKS
*CALL(PANEL,LOADS)
*XQT DCU
TOC 1
*XQT TAN
*XQT K
*XQT KG
*XQT AUS
KSHFT=SUM(K,"SHIFT" KG)
*XQT RSI
RESET K=KSHFT
*XQT EIG
RESET PROB=BUCK,NREQ=1,INIT=4
RESET SHIFT="SHIFT",K=KSHFT
*XQT DCU
TOC 1
COPY 1,2 BUCK EVAL
COPY 1,2 BUCK MODE
TOC 2
*RETURN
* ABC
```

Figure A7.- Listing of runstream PANEL, BUCK.

```
*(28,PANEL,LOADS) ABC
*XQTC U1
$
$ A GENERAL RUNSTREAM TO DIRECTLY APPLY A SET OF SPECIFIED
$ PRE-BUCKLING STRESS RESULTANTS TO A PRISMATIC STRUCTURE
$ COMPOSED OF REPEATING ELEMENTS.
$
$ INPUT DATA SETS :
$ EDEF REPE 1 1 - TABLE DEFINING ELEMENT CONNECTIVITY IN THE
$ CROSS SECTION OF THE REPEATING ELEMENT
$ STRESS TABLE 1 1 - TABLE DEFINING NX, NY, NXY VALUES FOR EACH
$ SA TYPE IN THE REPEATING ELEMENT
*REGISTER EXCEPTIONS=NREP, NMNX, NUMN
*REGISTER STORE(15 HOLD REG 1 1)
$ NREP - NUMBER OF REPEATING ELEMENTS
$ NMNX - NUMBER OF NODES IN THE LENGTH DIRECTION
$
!  NERE=TOC,NJ(1,EDEF,REPE,1,1)
!  NELX=NMNX-1
*XQT AUS
SYSVEC : STAT DISP
I=1,2,3,4,5,6 : J=1,"NUMN" : 0.  0.  0.  0.  0.  0.
ELDATA : DISL E43 1 1
$
$ LOOP OVER ALL REPEATING ELEMENTS IN THE STRUCTURE
$
!  IELT=1
!  CNT1=NREP
*LABEL RELOOP
$
$ LOOP OVER ALL ELEMENTS IN THE REPEATING ELEMENT
$
!  CNT2=NERE
!  JJ=1
*LABEL NELOOP
!  NSECT=DS,4,"JJ",1(1,EDEF,REPE,1,1)
!  NX=DS,1,"NSECT",1(1,STRES,TABL,1,1)
!  NY=DS,2,"NSECT",1(1,STRES,TABL,1,1)
!  NXY=DS,3,"NSECT",1(1,STRES,TABL,1,1)
!  IEL2 = IELT + NELX - 1
G=1 : E="IELT","IEL2"
"NX" 0.  "NY" 0.  "NXY" 0.  0.  0.  0.  0.  0.  0.  0.  0.  0.
!  JJ=JJ+1
!  IELT = IELT + NELX
*JGZ,-1(CNT2,NELOOP)
*JGZ,-1(CNT1,RELOOP)
*XQT DCU
CHANGE 1 DISL E43 1 1 KGF E43 1 1
*XQT GSF
RESET KGF=1
*XQT U1
*REGISTER RETRIEVE(15 HOLD REG 1 1)
*RETURN
* ABC
```

Figure A8.- Listing of runstream PANEL, LOADS.

REFERENCES

1. Wittrick, W. H.; and Williams, F. W.: Buckling and Vibration of Anisotropic or Isotropic Plate Assemblies Under Combined Loadings. Int. J. Mech. Sci., vol. 16, no. 4, Apr. 1974, pp. 209-239.

2. Anderson, Melvin S.; Hennessy, Katherine W.; and Heard, Walter L., Jr.: Addendum to Users Guide to VIPASA (Vibration and Instability of Plate Assemblies Including Shear and Anisotropy). NASA TM X-73914, 1976.

3. Williams, F. W.; and Anderson, M. E.: User's Guide to VIPASA (Vibration and Instability of Plate Assemblies Including Shear and Anisotropy). Dep. Civil Eng., Univ. of Birmingham, England, Jan. 1973.

4. Viswanathan, A. V.; Tamekuni, M.; and Tripp, Leonard L.: Elastic Stability of Biaxially Loaded Longitudinally Stiffened Composite Structures. AIAA J., vol. 11, no. 11, Nov. 1973, pp. 1553-1559.

5. Stroud, W. Jefferson; and Agranoff, Nancy: Minimum-Mass Design of Filamentary Composite Panels Under Combined Loads: Design Procedure Based on Simplified Buckling Equations. NASA TN D-8257, 1976.

6. Whetstone, W. D.: EISI/SPAR Reference Manual - System Level 103. Engineering Information Systems, Inc., Jan. 1979.

7. Whetstone, W. D.: EISI-EAL: Engineering Analysis Language. Proceedings of the Second Conference on Computing in Civil Engineering, American Soc. Civil Eng., 1980, pp. 276-285.

8. Almroth, B. O.; and Brogan, F. A.: The STAGS Computer Code. NASA CR-2950, 1978.

9. Almroth, B. O.; Brogan, F. A.; and Stanley, G. M.: Structural Analysis of General Shells - Volume II: User Instructions for STAGSC-1. NASA CR-165671, 1981.

10. Anderson, Melvin S.; and Stroud, W. Jefferson: General Panel Sizing Computer Code and Its Application to Composite Structural Panels. AIAA J., vol. 17, no. 8, Aug. 1979, pp. 892-897.

11. Stroud, W. Jefferson; and Anderson, Melvin S.: PASCO: Structural Panel Analysis and Sizing Code, Capability and Analytical Foundations. NASA TM-80181, 1981. (Supersedes NASA TM-80181, 1980.)

12. Anderson, Melvin S.; Stroud, W. Jefferson; Durling, Barbara J.; and Hennessy, Katherine W.: PASCO: Structural Panel Analysis and Sizing Code, User's Manual. NASA TM-80182, 1981. (Supersedes NASA TM-80182, 1980.)

13. Stroud, W. Jefferson; Greene, William H.; and Anderson, Melvin S.: Buckling Loads for Stiffened Panels Subjected to Combined Longitudinal Compression and Shear Loadings: Results Obtained With PASCO, EAL, and STAGS Computer Programs. NASA TM-83194, 1981.

14. Gallagher, Richard H.: Finite Element Analysis - Fundamentals. Prentice-Hall, Inc., c.1975.

15. Robinson, James C.; and Blackburn, Charles L.: Evaluation of a Hybrid, Anisotropic, Multilayered, Quadrilateral Finite Element. NASA TP-1236, 1978.

16. Timoshenko, Stephen P.; and Gere, James M.: Theory of Elastic Stability, Second ed. McGraw-Hill Book Co., 1961.

17. Becker, Herbert: Handbook of Structural Stability, Part II - Buckling of Composite Elements. NACA TN 3782, 1957.

18. Timoshenko, S.; and Woinowsky-Krieger, S.: Theory of Plates and Shells, Second ed. McGraw-Hill Book Co., Inc., 1959.

19. Anderson, M. S.; Williams, F. W.; and Wright, C. J.: Buckling and Vibration of Any Prismatic Assembly of Shear and Compression Loaded Anisotropic Plates With an Arbitrary Supporting Structure. Int. J. Mech. Sci., vol. 25, no. 8, 1983, pp. 585-596.

1. Report No.	2. Government Accession No.	3. Recipient's Catalog No.
NASA TP-2215		

4. Title and Subtitle	5. Report Date
BUCKLING LOADS OF STIFFENED PANELS SUBJECTED TO COMBINED LONGITUDINAL COMPRESSION AND SHEAR: RESULTS OBTAINED WITH PASCO, EAL, AND STAGS COMPUTER PROGRAMS	January 1984
	6. Performing Organization Code: 534-03-23-07
7. Author(s): W. Jefferson Stroud, William H. Greene, and Melvin S. Anderson	8. Performing Organization Report No.: L-15630
	10. Work Unit No.
9. Performing Organization Name and Address: NASA Langley Research Center, Hampton, VA 23665	11. Contract or Grant No.
	13. Type of Report and Period Covered: Technical Paper
12. Sponsoring Agency Name and Address: National Aeronautics and Space Administration, Washington, DC 20546	14. Sponsoring Agency Code

15. Supplementary Notes

16. Abstract

Buckling analyses used in PASCO are summarized with emphasis placed on the shear buckling analyses. PASCO buckling analyses include the basic VIPASA analysis, which is essentially exact for longitudinal and transverse loads, and a smeared stiffener solution, which treats a stiffened panel as an orthotropic plate. Buckling results are then presented for seven stiffened panels loaded by combinations of longitudinal compression and shear. The buckling results were obtained with the PASCO, EAL, and STAGS computer programs. The EAL and STAGS solutions were obtained with a fine finite element mesh and are very accurate. These finite element solutions together with the PASCO results for pure longitudinal compression provide benchmark calculations to evaluate other analysis procedures. For each example, several figures illustrate buckling mode shapes for pure compression and pure shear loading.

17. Key Words (Suggested by Author(s))		18. Distribution Statement
Stiffened panels	Stringers	Unclassified - Unlimited
Panels	Optimization	
Stiffening	Rectangular panels	
Buckling	Composite structures	Subject Category 39
Reinforced plates		

19. Security Classif. (of this report)	20. Security Classif. (of this page)	21. No. of Pages	22. Price
Unclassified	Unclassified	77	A05

For sale by the National Technical Information Service, Springfield, Virginia 22161

NASA-Langley, 1984